

Journal of Visualized Experiments

Control of cell geometry through infrared laser assisted micropatterning

--Manuscript Draft--

| | |
|---|---|
| Article Type: | Methods Article - Author Produced Video |
| Manuscript Number: | JoVE62492R2 |
| Full Title: | Control of cell geometry through infrared laser assisted micropatterning |
| Corresponding Author: | Sergey V Plotnikov, PhD University of Toronto Toronto, Ontario CANADA |
| Corresponding Author's Institution: | University of Toronto |
| Corresponding Author E-Mail: | sergey.plotnikov@utoronto.ca |
| Order of Authors: | Shuying Yang Chen Tuo Ernest lu Sergey V Plotnikov, PhD |
| Additional Information: | |
| Question | Response |
| Please indicate whether this article will be Standard Access or Open Access. | Standard Access (US\$1200) |
| Please specify the section of the submitted manuscript. | Bioengineering |
| Please confirm that you have read and agree to the terms and conditions of the author license agreement that applies below: | I agree to the Author License Agreement |
| Please provide any comments to the journal here. | |
| Please indicate whether this article will be Standard Access or Open Access. | Standard Access (\$1400) |

TITLE:

Control of Cell Geometry through Infrared Laser Assisted Micropatterning

AUTHORS AND AFFILIATIONS:

Shuying Yang¹, Chen Tuo¹, Ernest Iu¹, Sergey V Plotnikov¹

¹Department of Cell and Systems Biology, University of Toronto, Ontario, Canada

Email addresses of authors:

Shuying Yang (rosiey.yang@mail.utoronto.ca)

Chen Tuo (chen.tuo@mail.utoronto.ca)

Ernest Iu (ernest.iu@mail.utoronto.ca)

Corresponding author:

Sergey V Plotnikov (sergey.plotnikov@utoronto.ca)

SUMMARY:

The protocol presented here enables automated fabrication of micropatterns that standardizes cell shape to study cytoskeletal structures within mammalian cells. This user-friendly technique can be set up with commercially available imaging systems and does not require specialized equipment inaccessible to standard cell biology laboratories.

ABSTRACT:

Micropatterning is an established technique in the cell biology community used to study connections between the morphology and function of cellular compartments while circumventing complications arising from natural cell-to-cell variations. To standardize cell shape, cells are either confined in 3D molds or controlled for adhesive geometry through adhesive islands. However, traditional micropatterning techniques based on photolithography and deep UV heavily depend on clean rooms or specialized equipment. Here we present an infrared laser assisted micropatterning technique (microphotopatterning) modified from Doyle et al. that can be conveniently set up with commercially available imaging systems. In this protocol, we use a Nikon A1R MP+ imaging system to generate micropatterns with micron precision through an infrared (IR) laser that ablates preset regions on poly-vinyl alcohol coated coverslips. We employ a custom script to enable automated pattern fabrication with high efficiency and accuracy in systems not equipped with a hardware autofocus. We show that this IR laser assisted micropatterning (microphotopatterning) protocol results in clear patterns to which cells attach exclusively and take on the desired shape. Furthermore, data from a large number of cells can be averaged due to the standardization of cell shape. Patterns generated with this protocol, combined with imaging and analysis, can be used for relatively high throughput screens to understand molecular players mediating the link between form and function.

INTRODUCTION:

Cell shape is a key determinant of fundamental biological processes such as tissue morphogenesis¹, cell migration², cell proliferation³, and gene expression⁴. Changes in cell shape

are driven by an intricate balance between dynamic rearrangements of the cytoskeleton that deforms the plasma membrane and extrinsic factors such as external forces exerted on the cell and the geometry of cell-cell and cell-matrix adhesions⁵. Migrating mesenchymal cells, for instance, polymerize a dense actin network at the leading edge that pushes the plasma membrane forward and creates a wide lamellipodia⁶, while actomyosin contractility retracts the cell's narrow trailing edge to detach the cell from its current position^{7, 8}. Disrupting signaling events that give rise to such specialized cytoskeletal structures perturbs shape polarity and slows cell migration⁹. In addition, epithelial sheet bending during gastrulation requires actomyosin-based apical constriction that causes cells and their neighbors to become wedge-shaped¹⁰. Although these studies highlight the importance of cell shape, the inherent heterogeneity in cell shape has encumbered efforts to identify mechanisms that connect morphology to function.

To this end, numerous approaches to manipulate cell shape have been developed over the past three decades. These approaches achieve their goal by either constraining the cell with a three-dimensional mold or controlling cellular adhesion geometry through patterned deposition of extracellular matrix (ECM) proteins onto an antifouling surface, a technique termed micropatterning¹¹. Here we will review a number of techniques that have gained popularity throughout the years.

Originally pioneered as an approach for microelectronic applications, soft lithography-based microcontact printing¹² has unequivocally become a cult favorite. A master wafer is first fabricated by selectively exposing areas of a photoresist-coated silicon substrate to photoirradiation¹³, leaving behind a patterned surface. An elastomer, such as PDMS, is then poured onto the master wafer to generate a soft "stamp" that transfers ECM proteins to a desired substrate^{11, 14}. Once fabricated, a master wafer can be used to cast many PDMS stamps that give rise to highly reproducible micropatterns¹². However, the patterns cannot be readily adjusted on demand due to the lengthy photolithography process. This process also requires highly specified equipment and cleanrooms that are not typically available in Biology departments.

More recently, direct printing using deep UVs has been reported to circumvent limitations posed by traditional lithography-based approaches. Deep UV light is directed through a photomask to selective areas of a glass coverslip coated with poly-L-lysine-*grafted*-polyethylene glycol. Chemical groups exposed to deep UV are photoconverted without the use of photosensitive linkers to enable binding of ECM proteins¹⁵. The lack of photosensitive linkers enables patterned coverslips to remain stable at room temperature for over seven months¹⁵. This method avoids the use of cleanrooms and photolithography equipment and requires less specialized training. However, the requirement for photomasks still poses a substantial hurdle for experiments that require readily available changes in patterns.

In addition to methods that manipulate cell geometry through controlled deposition of ECM proteins on a 2D surface, other seek to control cell shape by confining cells in 3D microstructures. Many studies have adapted the soft lithography-based approach described above to generate 3D, rather than 2D, PDMS chambers to investigate shape-dependent biological processes in embryos, bacteria, yeast and plants^{16–19}. Two-photon polymerization (2PP) has also taken the

lead as a microfabrication technique that can create complex 3D hydrogel scaffolds with nanometer resolution²⁰. 2PP relies on the principles of two-photon adsorption, where two photons delivered in femtometer pulses are absorbed simultaneously by a molecule – photoinitiator in this case – that enables local polymerization of photopolymers²¹. This technique has been heavily employed to print 3D scaffolds that mimic the native ECM structures of human tissue and has been shown to induce low photochemical damage to cells²².

The debut of microphotopatterning 10 years ago gave researchers the opportunity to fabricate micropatterns while avoiding inaccessible and specialized equipment. Microphotopatterning creates patterns on the micron scale by thermally removing selective regions of poly-vinyl alcohol (PVA) coated on activated glass surfaces using an infrared (IR) laser^{23, 24}. ECM proteins that attach only the underlying glass surface and not PVA then serve as biochemical cues to enable controlled spreading dynamics and cell shape. This method also offers superior flexibility since patterns can be readily changed in real time. Here, we provide a step-by-step protocol of microphotopatterning by using a commercial multi-photon imaging system. The described protocol is designed for rapid and automated fabrication of large patterns. We demonstrated that these patterns efficiently control cell shape by constraining the geometry of cell-ECM adhesions. Finally, we demonstrate that the described patterning technique modulates the organization and dynamics of the actin cytoskeleton.

PROTOCOL:

1. Coverslip preprocessing

1.1. Prepare squeaky-clean coverslips as described in Waterman-Storer, 1998²⁵.

1.2. Prepare 1% (3-aminopropyl)trimethoxysilane (APTMS) solution and incubate the coverslips in the solution for 10 min with gentle agitation. Make sure that coverslips move freely in the solution.

1.3. Wash coverslips twice with dH₂O for 5 min each.

1.4. Prepare 0.5% glutaraldehyde (GA) solution and incubate the coverslips in the solution for 30 min on a shaker. For 25 coverslips, use 50 mL of glutaraldehyde solution. Make sure that coverslips move freely in the solution.

1.5. Wash coverslips three times with dH₂O for 10 min each.

1.6. Spin dry coverslips for 30 s using a custom-built coverslip spinner. A detailed description of the coverslip spinner has been published²⁶ and is available online (<https://mullinslab.ucsf.edu/home-built-coverslip-drierspinner/>). Activated coverslips can be stored for up to one month at +4 °C in a box with dividers so that they stand apart from each other.

2. PVA coating

2.1. Mix PVA (98% hydrolyzed PVA, MW 98000) with dH₂O to make a 5.6% solution.

2.2. Solubilize the mixture in a 90 °C water bath and immediately filter through a 0.2 µm filter in a biosafety cabinet while hot. Filter the stock solution again if it precipitates. PVA solution can be stored at room temperature for 3 months.

2.3. In a 15 mL tube, add one part HCl to eight parts PVA. Invert the tube carefully a few times to mix.

2.4. Pour 2 mL of the mixed solution into a 35 mm Petri dish and submerge a clean, preprocessed coverslip into the liquid, taking care that the coverslips do not stick to the bottom. Incubate at room temperature for 5 min on a shaker.

2.5. Carefully remove the coverslips from the solution. Use the coverslip spinner to spin coat for 40 s. In the meantime, clean the tweezers. Transfer the coverslip to a box and dry at +4 °C overnight. PVA-coated coverslips can be stored at +4 °C for up to two weeks.

3. Configuring the Multiphoton Microscope

NOTE: The described protocol is tuned up to create cell adhesive micropatterns of desired shape and size on upright or inverted multi-photon imaging systems, especially the ones that are not equipped with a hardware autofocus. Thus, for every field of view (FOV), the patterning script ablates a small area to create a fiduciary marker on the coverslip, uses a software autofocus to focus the microscope on the coverslip surface, and ablates the desired pattern. Running this script in a loop for adjacent FOVs robustly creates a large array of micropatterns (5 x 5 mm or larger) that constrain cell shape and modulate the activity of intracellular biological processes. The described protocol was developed for Nikon A1R MP+ imaging system controlled by NIS-Elements software. If an imaging system from another vendor is used for patterning, the optical configurations and patterning script should be adjusted according to the manufacturer's instructions.

3.1. Turn on the microscope software. Ensure that the "Apo LWD 25X/1.10W DIC N2" objective is mounted on the microscope.

NOTE: The protocol described here is optimized for a 25x/1.1 NA water immersion objective, but other objectives can also be used for patterning. Readers should be aware that patterning with a high-magnification objective (*e.g.*, 40x and 60x) takes longer time as it significantly decreases the number of patterns ablated in each FOV. Low magnification objectives can be used for patterning as long as they provide uniform illumination across the FOV and laser power sufficient to ablate the PVA layer.

3.2. In the "A1plus MP GUI" window, set the laser line to 750 nm.

3.3. Setting up the “Image” optical configuration

NOTE: NIS-Elements provides users with several tools (graphical interface, an acquisition workflow builder JOBS, optical configurations, and macros) to control the microscope hardware. In this protocol, most of the hardware control is achieved through various optical configurations as well as ND Acquisition and ND Stimulation modules.

3.3.1. In the **Calibration** tab, click on **New Optical Configuration**. Name the optical configuration “Image”. This is the baseline optical configuration that allows imaging of the coverslip through reflectance. Leave all other options as default and select the appropriate objective.

3.3.2. In the **A1plus MP GUI** window, click on the **Settings** button to configure the hardware settings under this optical configuration. Set the **Stimulation laser** to **IR stim**, place the beam splitter (BS 20/80) in the light path, set the **Scanner Unit** to **Galvano** and select the appropriate descanned detector.

3.3.3. In the **A1plus Compact GUI** window, select a scan size and dwell time that is sufficient to capture small features on the coverslip (1.1 ms and 1024 pixels on our system, respectively). Click on the **Normal** button so no line averaging or line integration is performed. Make sure the **Use IR laser** box is checked. Set up unidirectional scanning for simplicity.

NOTE: If scan speed is of concern, bidirectional scanning can be used.

3.3.4. In the same window, adjust laser power and detector sensitivity to obtain bright but not saturated image of the coverslip surface. Setting laser power to 3 – 5% of the maximum power and detector sensitivity (“HV” slider) to 15 V is a good starting point.

3.3.5. In the **A1plus Scan Area** window, set zoom to 1 to capture the entire FOV.

3.3.6. Save the optical configuration.

3.4. Setting up the “Print_Fudiciary_Marker” optical configuration

3.4.1. Duplicate the “Image” optical configuration and rename it “Print_Fudiciary_Marker”.

3.4.2. In the **A1plus Compact GUI** window, select the smallest scan size and dwell time (64 pixels and 80.2 ms on our system, respectively).

3.4.3. Since no imaging is required in this step, set detector sensitivity to 0 and increase laser power to 30%. Higher laser power will thermally remove the PVA layer on the coverslip in the desired regions.

3.4.4. In the **A1plus Scan Area** window, set **Zoom** to maximum (15.87 for our system) and place the scan area in the middle of the FOV.

3.4.5. In the **ND Acquisition** window, set up a Z-stack experiment. Set movement in the Z position to **Relative** and select the appropriate Z device. Set the step size to 2 μm and the stack depth to 10 μm above and below to account for any unevenness in the microscope stage or the PVA surface between adjacent FOVs.

3.5. Setting up the “Autofocus” optical configuration

3.5.1. Duplicate the “Image” optical configuration and rename it “Autofocus”.

3.5.2. In the **A1plus Scan Area** window, decrease the **Zoom** factor so the FOV is slightly larger than the fiduciary marker. This ensures that other small features on the coverslip will not interfere with autofocusing.

3.5.3. In the **Devices** menu, select **Autofocus Set Up**. Set the scan thickness to that of the Z-stack in the Z-stack experiment (see step 3.5.5). The microscope will scan through this range and find the best focal plane using the fiduciary marker. Leave the step size as default.

3.6. Setting up the “Load_ROI” optical configuration

3.6.1. Duplicate the “Image” optical configuration and rename it “Load_ROI”.

3.6.2. In the **A1plus Compact GUI** window, set scan size identical to that of the ROI mask. This optical configuration will be used to capture an image onto which the ROI mask will be loaded. We used 2048 pixels to achieve an optimal balance between resolution and speed.

NOTE: It is essential that this captured image is identical in size to the ROI mask.

3.7. Setting up the “Micropattern” optical configuration

3.7.1. Duplicate the “Print_Fiduciary_Marker” optical configuration and rename it “Micropattern”.

3.7.2. Set the **Zoom** factor to one.

3.7.3. In the **A1plus MP GUI** window, increase the stimulation laser power to ablate PVA and select an appropriate scan speed (40% and 32 s/frame in our experiments, respectively).

3.7.4. In the **ND Stimulation** window, set up a ND stimulation experiment. Add a few phases to the **Time Schedule** and set each as **Stimulation**. Ensure stimulation area and duration are correct.

NOTE: The number of phases can be adjusted according to the thickness and smoothness of the PVA layer as well as the laser power used in this optical configuration.

3.7.5. In the same window, enable the the **StgMoveMainZ(-1.000,1)** function before each phase. This again accounts for any deviations in the Z-direction.

NOTE: The distance and direction in which the objective moves can be adjusted according to the thickness and smoothness of the PVA layer.

3.8. Setting up the “Label_Surface” optical configuration

3.8.1. Duplicate the “Print_Fudiciary_Marker” optical configuration and rename it “Label_Surface”.

3.8.2. In the **A1plus Compact GUI** window, increase laser power significantly and set Zoom to one. High laser power used here will physically damage the glass coverslip and produce a label visible to the naked eye. This aids in locating the patterns in further experiments.

4. Generating the ROI mask and Setting up the macro

4.1. Generating the ROI mask

4.1.1. Use Adobe Photoshop or other available software to generate a 2048 × 2048 RGB image. The image corresponds to a FOV under the microscope (*i.e.*, 532.48 × 532.48 μm, 0.26 μm per pixel). The image should have a black (0, 0, 0) background.

NOTE: A number of commercial and free image editors can be used to generate ROI masks for laser assisted micropatterning. Although we use Adobe Photoshop to generate the masks, GIMP and ImageJ/Fiji are also available as alternative free option.

4.1.2. Draw 8 – 12 white (255,255,255) patterns on the black background. Pattern size varies depending on cell type (~200 pixels in diameter). Leave a 500 × 500 blank area in the center of the image for autofocusing. Leave sufficient space between adjacent patterns (>200 pixels) and at the boarder of the FOV for optimal ablation and cell attachment. Patterns presented in this protocol are available on Github (<https://github.com/PlotnikovLab/Micropatterning>).

4.2. Setting up the macro

4.2.1. Click on the **Macro** menu and select **New Macro**.

4.2.2. Import the “Pattern_Stimulation” code available on Github (<https://github.com/PlotnikovLab/Micropatterning>) into the **New Macro** window. Save this piece of code to an appropriate folder.

4.2.3. Open another **New Macro** window and import the “Stage_Movement” code available on Github (<https://github.com/PlotnikovLab/Micropatterning>). Ensure that the “Stage_Movement” working directory in this code is identical to that in step 4.2.2. Save the “Stage_Movement” code to the same folder in step 4.2.2.

5. Generating micropatterns using photo ablation

5.1. Turn on the microscope and its accessories. Ensure that the IR laser has warmed up sufficiently prior to this.

5.2. Transfer the PVA-coated coverslip onto a holder. For an upright microscope, ensure the PVA surface to be ablated faces down.

5.3. Add water to the corners to stabilize the coverslip and mount the holder onto the microscope stage.

5.4. Lower the objective and add water onto the coverslip.

NOTE: The protocol described here is optimized for a 25x/1.1 NA water immersion objective. If a dry or oil immersion objective is used, water should be replaced with an appropriate immersion media. When a water immersion objective is used to generate a large micropattern array, evaporation might become an issue. If this is the case, water should be replaced with GenTeal, an over-the-counter eye lubricant available from pharmacies.

5.5. In the microscope software, turn on the IR laser shutter in the “A1plus MP GUI” window. Click on the **Autoalignment** button to align the laser prior to patterning.

NOTE: It is crucial to perform laser autoalignment at the beginning of each patterning session as small deviations in the laser path will significantly affect the quality of the patterns.

5.6. Switch to the “Image” optical configuration. In the **A1plus Compact GUI** window, click **Scan** to scan the FOV while slowly moving the objective closer to the coverslip.

5.7. Carefully monitor the image. At first, the image will appear extremely dim. Move the objective closer to the coverslip until the image brightness increases. This is the coverslip surface that is facing the objective. Continue to move the objective until the brightness decreases and increases again. This is the PVA surface to be patterned. Focus on any small feature (coverslip imperfections, dust, etc.) on this surface and set zero on the Z drive. Always set zero after focusing.

NOTE: Although both surfaces of the coverslip are coated with PVA, the optical properties are not significantly altered. We routinely image such coverslips with dry, water- and oil-immersion objectives and did not find the non-patterned PVA surface to interfere with imaging.

5.8. Switch to the “Label_Surface” optical configuration. Click on **Capture**. Return to **Imaging** and scan. The glass surface should be damaged and appear amorphous. The damaged area is visible to the naked eye, indicating the location of patterns in further experiments.

NOTE: To increase the size of the visible label, repeat step 5.8 in multiple adjacent FOVs.

5.9. Check again that the objective is roughly in the center of the coverslip. Ensure that there is sufficient water between the objective and the coverslip. Move the stage by 1 to 2 FOVs to avoid glass particles and scan to confirm.

5.10. In the **Devices** menu, open the **Stage_Movement** macro. Check that the **Pattern_Stimulation** working directory is correct; if not, stimulation will not occur. Set the variables “m” and “n” to the desired number of FOVs that will be patterned. Save and run the macro.

5.11. After patterning is complete, switch to the “Imaging” optical configuration. Again, check that the IR laser shutter is open in the **A1plus MP GUI** window.

5.12. Move the stage to view the patterns. Scan through the patterns to check their quality.

5.13. Transfer the coverslip to the grid box, with patterns facing up.

5.14. Store patterned coverslips at +4 °C for up to one week before use.

6. Fibronectin adsorption

6.1. Make fresh 1 M NaBH₄ in 1 M NaOH solution. Add at a 1:100 ratio to pH 8.0 phosphate buffer containing 0.2 M ethanolamine.

6.2. Transfer patterned coverslips to a 35 mm tissue culture dish. Incubate each coverslip with 1 mL of the solution above for 8 min to quench autofluorescence, and then rinse 3 times with PBS.

6.3. Dilute fibronectin (FN) in PBS to a final concentration of 10 µg/mL. Incubate the coverslip in FN for 1 h at +37 °C.

NOTE: If substantial nonspecific binding of ECM protein to the substrate is observed, FN can be diluted in PBS containing 0.1% Pluronic F-127²⁴.

6.4. Wash the coverslip 2 times with PBS. If not immediately used, store in PBS at +4 °C overnight.

7. Cell attachment

NOTE: The following protocol is optimized for primary human gingival fibroblasts.

7.1. Culture a 10 cm dish of cells to 70% confluency.

7.2. Warm up cell culture media, PBS and 0.05% trypsin in a +37 °C water bath.

NOTE: For cells that adhere weakly to the substrate, non-proteolytic dissociation with versene (0.48 mM EDTA) or a proprietary enzyme-free buffer may increase cell attachment to the patterns and should be considered.

7.3. Prior to seeding cells, relocate the patterned coverslip to a clean 35 mm tissue culture dish containing 1 mL warm PBS.

7.4. Aspirate the cell culture media from the 10 cm tissue culture dish and wash once with PBS.

7.5. Add 700 µL of 0.05% trypsin/EDTA to the dish and incubate cells in a +37 °C, 5% CO₂ incubator for 1 min.

7.6. In the meantime, aspirate the PBS covering the patterned coverslip and add 1 mL of cell culture media.

7.7. Confirm that cells have detached. Then resuspend the trypsinized cells with 10 mL of cell culture media and add 1 mL to the patterned coverslip.

7.8. Culture cells in the incubator for 2 – 3 h and check if a sufficient number of cells have attached to the patterns. If so, change media once to remove unattached cells. This minimizes the chance of multiple cells landing on the same pattern.

NOTE: Attachment time may vary depending on cell type.

7.9. After another 3-4 h, or when a sufficient number of cells have spread on patterns, cells are ready for further experiments. Do not wait for too long to avoid cell division.

8. Data acquisition

8.1. Fix cells with 4% PFA in cytoskeleton buffer²⁷ for 10 min at room temperature.

8.2. Follow immunofluorescence protocols established for the proteins of interest. PVA-coated coverslips work well with any immunofluorescence protocol.

8.3. Acquire images of cells using an appropriate microscope. Depending on the goal of the experiment, image either one or multiple cells per FOV.

9. Image analysis

NOTE: The following protocol allows users to obtain the average fluorescence signal of the protein of interest over a large number of cells from Z-stacks of microscope images.

9.1. Open the acquired images in NIS Elements and crop the images. Ensure that each image contains only one well-spread cell. Detailed instructions on image processing can be found in the script below.

9.2. Install Anaconda and launch Spyder through Anaconda Navigator.

NOTE: The .py scripts can be run in any environment with the appropriate packages identified in the requirements.txt file installed. We recommend Anaconda because it contains most of the required packages for the codes below.

9.3. Download the script from Github (<https://github.com/PlotnikovLab/Micropatterning>) and open in Spyder ("Pattern_Averaging_3Channels.py" or "Pattern_Averaging_4Channels.py" for images with 3 Channels or 4 Channels, respectively).

9.4. Set parameters based on the acquired images. See the script for detailed descriptions.

9.5. Press **F5** to run the script. The progress can be tracked in the Console panel.

9.6. Retrieve the output files saved in the same folder. The output images are the average of each channel for all samples. The excel sheet shows the mean intensity of each channel within a sample cell, which enables further quantitative analysis.

REPRESENTATIVE RESULTS:

The quality of the experimental data obtained with a micropatterning technique is largely dependent on the quality of the patterns. To determine the quality of patterns generated with the method above, we first used reflectance microscopy to assess the shape and size of the photo ablated areas of the coverslip. We found that each individual pattern looked very similar to the ablation mask and displayed clear borders and a surface that reflected light uniformly (**Figure 2B**). A variety of shapes and sizes can be printed depending on the desired cytoskeleton architecture, but we used the crossbow shape that best suits our purposes. Atomic force microscopy (AFM) revealed that such patterns were approximately 140 nm in height and had a smooth surface with minimal topological variation throughout (**Figure 2F**). Suboptimal patterning settings, such as low laser power and incorrect focal plane, resulted in incomplete removal of the PVA surface that manifests as darker, partial patterns with uneven topology (**Figure 2C**). Setting laser power too high resulted in PVA "bubbling" and when extreme, coverslip surface damage that is also undesirable (**Figure 2D**).

In preliminary experiments we attempted to increase the patterning area by abating multiple FOVs on a single coverslip. We found that this approach, although works in principle, is unreliable

and tedious due to Z-drift of the microscope stand and slight tilt of the coverslip. To achieve high-quality patterns over a large number of FOVs in an automated fashion, we implemented a customized macro that improved the precision of microscope focusing during the patterning process. The multiphoton microscope employs a pulse laser that efficiently degrades PVA with high power in a narrow focal plane, making the patterning process sensitive to any unevenness or tilt in the sample. As a result, it is important to identify the precise focal plane in each FOV. This is even more problematic for systems lacking a perfect focus module, as deviations as little as one to two microns can render the patterning process fruitless. To address this problem, the customized macro script first patterns a small square in the center of each new FOV that is only roughly in focus by scanning through a relatively thick Z-stack ($\approx 20\ \mu\text{m}$). The microscope then quickly scans through the stack of images and uses NIS Elements autofocus function to identify the optimal focal plane. The pattern mask is then loaded and set as stimulation ROI for IR stimulation to occur. The stage subsequently moves to the next FOV and repeats this process. In addition, the square-wave shaped path of the microscope stage movement ensured minimal error accumulation between sequential FOVs. By using this protocol, we routinely fabricate patterns composed of 49 microscope FOVs covering $3.5 \times 3.5\ \text{mm}$ area of the coverslip in less than 3 h.

To test if patterned areas, not unperturbed PVA, could adsorb ECM proteins, we coated patterned coverslips with $10\ \mu\text{g}/\text{mL}$ FN and stained them with anti-FN antibody. Using wide field fluorescent microscopy, we found that FN uniformly adsorbed to the patterned areas where PVA had been removed by laser degradation (**Figure 2E**).

To determine if cytoskeleton architecture and tension distribution could be modified as expected on the patterns, we seeded cells on patterned coverslips and visualized the distribution of myosin light chain, a marker of contractility, through fluorescence microscopy. After initial seeding, cells gradually gravitated towards the coverslip. Those that landed on patterned areas attached and spread into the shape of the pattern over time. Those that landed on PVA only loosely attached and were removed after several washes and media changes. We found that cells spread on patterns displayed phenotypical fibroblast structures including an actin-dense rim of lamellipodia, thick ventral stress fibers along the two sides, and dorsal stress fibers emanating from the lamellipodia connected by transverse arcs (**Figure 3A**). Myosin light chain (MLC) sat behind the dense lamellipodia rim and displayed a striated pattern along actin bundles. As indicated by averaged images of many cells, this phenotype was consistent across a large number of patterns (**Figure 3B**).

FIGURE AND TABLE LEGENDS:

Figure 1. Schematic of IR laser assisted micropatterning (microphotopatterning). (A) Glass coverslips are chemically coated with APTMS, GA and PVA, in the respective order. The PVA surface is non-adhesive to cells and proteins. (B) PVA is removed in preset patterns by an IR laser. (C) Patterned coverslips are coated with ECM protein that will only adsorb to patterned areas. (D) Cells are plated on coverslips, fixed, and immunostained for proteins of interest. Cells that land on patterned islands spread into the shape of the pattern that gives rise to characteristic cytoskeletal structures, while those that land on PVA remain spherical.

Figure 2. Micropattern validation and characterization. (A) IR laser assisted micropatterning (microphotopatterning) setup on a microscope stage. The IR laser thermally ablates PVA in multiple FOVs. (B) A reflectance microscopy image of micropatterns that have clear borders and are identical to the ROI masks. (C) A reflectance microscopy image of incomplete removal of PVA resulting from suboptimal laser power. (D) A reflectance microscopy image of PVA bubbling and (corners) and coverslip surface damage resulting from excess laser power. (E) Immunofluorescence images of FN coated patterned coverslips stained with anti-FN primary antibodies and fluorophore-conjugated secondary antibodies. (F) An AFM topology scan line and a representative AFM image of a crossbow pattern. To measure the topology of the micropattern, contact mode imaging was performed using a Bruker AFM probe (MLCT-B) mounted on a NanoWizard 4 atomic force microscope.

Figure 3. Representative images of cells plated on micropatterns. (A) Representative images of a primary human gingival fibroblast plated on crossbow patterns immunostained for actin and MLC. Images were acquired with a confocal microscope and a 100x objective. (B) Averaged immunofluorescence images of actin and MLC in cells plated on crossbow patterns generated by a custom Python script.

DISCUSSION:

The results above demonstrate that the described IR laser assisted micropatterning (microphotopatterning) protocol provides reproducible adherent patterns of various shapes that enables the manipulation of cell shape and cytoskeletal architecture. Although numerous micropatterning methods have been described both prior to and after the debut of microphotopatterning, this method possesses several advantages. First, it does not require specialized equipment and cleanrooms that are usually only found within Engineering departments. In fact, as multiphoton microscopes are becoming a more common sight in Biology departments, microphotopatterning expands the applications of the multiphoton microscope and adds to the potential pool of users. Patterns can also be changed on demand with commercially available software, such as Photoshop and ImageJ, and printed immediately, instead of having to fabricate a new master wafer that entails a lengthy lithography process.

Compared to the pre-existing microphotopatterning protocol, one improvement in our protocol is the elimination of several time-consuming curing steps during coverslip preparation. We show that the quality of PVA-coverslip attachment remains unperturbed as the patterns were still intact and could bind cells even two weeks after fabrication. More importantly, we improved automation of the patterning process by eliminating the need to preset the position of each FOV²⁴. Instead, we implement an understandable macro that allows patterning of a large area while precisely identifying the optimal focal plane of each FOV.

Although the macros in the protocol enable automation of patterning on our system, we understand that every commercial laser scanning microscope comes with their own proprietary software that is rarely compatible with others, making it difficult to implement our exact protocol on other systems. However, the overall workflow can be well adapted to other commercial

systems to facilitate automated micropatterning, namely the process of focusing on each individual FOV, loading the mask, ablating PVA, and moving the microscope stage to a new FOV.

Several steps in the patterning protocol should be undertaken with great care to ensure efficient patterning. The most critical step is to optimize stimulation conditions before generating patterns. In multi-photon microscopy, two or more photons must arrive almost simultaneously at a fluorescent molecule and combine their energy to excite fluorescence. This low probability event creates an extremely thin optical section that increases signal-to-noise ratio²⁸. Although beneficial for imaging, this feature makes the removal of the thin PVA coating extremely sensitive to the sample's Z-position. Several measures can be implemented to counter this. First, laser power should be fine-tuned to ensure thorough removal of PVA without "boiling" the polymer or damaging the glass coverslip. If PVA removal is consistently incomplete, we recommend checking laser alignment as this usually increases laser power. Second, the microscope stage should be leveled to avoid sample tilt, which could result in incomplete patterns. IR stimulations in multiple Z-positions should also be set up to ensure that the PVA layer is targeted. Alternatively, if the microscope is equipped with a perfect focus module, preliminary tests can be conducted to determine the optimal offset in Z-position for PVA targeting. Another critical step is to set up a microscope macro that allows pattern stimulation in an automated fashion. The macro should find the focal plane of each new FOV to avoid complications from sample tilt or surface unevenness. It should also allow the stage to move in an S-shape from row to row, analogous to the path taken in bi-directional scanning, to minimize deviations in Z between consecutive FOVs.

One limitation to the protocol described is the time required to produce a large number of patterned coverslips, an unparalleled advantage offered by lithography-based microcontact printing^{29, 30}. As a result, this protocol is best suited for experiments in which a limited number of conditions are required, or those that require readily available adjustments in pattern shape and size. Furthermore, for systems lacking a hardware autofocus module, we integrate a series of stimulation events in different z-planes to ensure automated and effective PVA removal. Since IR stimulation is the most time-consuming step, the addition of each stimulation event (~30 sec) significantly lengthens the patterning process. If time is of concern, we suggest fine tuning autofocus by decreasing step size. This facilitates the identification of the best focal plane which will decrease the number of IR stimulation events required. In our experiments, decreasing the number of stimulation events from five to two reduces the time by half (1.5 h).

In conclusion, the IR laser assisted micropatterning (microphotopatterning) protocol we describe can be used in any lab that has access to an IR laser-equipped microscope. In addition to studying cytoskeletal architecture and signaling pathways that connect form to function, this technique can also be applied to drug screening and other applications that are sensitive to cell-to-cell variability.

ACKNOWLEDGMENTS:

This work was supported by Connaught Fund New Investigator Award to S.P., Canada Foundation for Innovation, NSERC Discovery Grant Program (grants RGPIN-2015-05114 and RGPIN-2020-05881), University of Manchester and University of Toronto Joint Research Fund, and University

of Toronto XSeed Program. C.T. was supported by NSERC USRA fellowship.

DISCLOSURES:

The authors disclose no conflict of interests.

REFERENCES:

1. Harris, T.J.C., Sawyer, J.K., Peifer, M. How the Cytoskeleton Helps Build the Embryonic Body Plan Models of Morphogenesis from Drosophila. *Current Topics in Developmental Biology*. **89**, 55–85, doi: 10.1016/s0070-2153(09)89003-0 (2009).
2. Keren, K. *et al.* Mechanism of shape determination in motile cells. *Nature*. **453** (7194), 475–480, doi: 10.1038/nature06952 (2008).
3. Castor, L.N. Control of Division by Cell Contact and Serum Concentration in Cultures of 3T3 Cells. *Experimental Cell Research*. **68** (1), 17–24, doi: 10.1016/0014-4827(71)90581-7 (1971).
4. Jain, N., Iyer, K.V., Kumar, A., Shivashankar, G.V. Cell geometric constraints induce modular gene-expression patterns via redistribution of HDAC3 regulated by actomyosin contractility. *Proceedings of the National Academy of Sciences*. **110** (28), 11349–11354, doi: 10.1073/pnas.1300801110 (2013).
5. Paluch, E., Heisenberg, C.-P. Biology and Physics of Cell Shape Changes in Development. *Current Biology*. **19** (17), R790–R799, doi: 10.1016/j.cub.2009.07.029 (2009).
6. Pollard, T.D., Borisy, G.G. Cellular Motility Driven by Assembly and Disassembly of Actin Filaments. *Cell*. **112** (4), 453–465, doi: 10.1016/s0092-8674(03)00120-x (2003).
7. Ridley, A.J. *et al.* Cell Migration: Integrating Signals from Front to Back. *Science*. **302** (5651), 1704–1709, doi: 10.1126/science.1092053 (2003).
8. Cramer, L.P. Mechanism of cell rear retraction in migrating cells. *Current Opinion in Cell Biology*. **25** (5), 591–599, doi: 10.1016/j.ceb.2013.05.001 (2013).
9. Lee, J., Ishihara, A., Oxford, G., Johnson, B., Jacobson, K. Regulation of cell movement is mediated by stretch-activated calcium channels. *Nature*. **400** (6742), 382–386, doi: 10.1038/22578 (1999).
10. Leptin, M. Gastrulation Movements: the Logic and the Nuts and Bolts. *Developmental Cell*. **8** (3), 305–320, doi: 10.1016/j.devcel.2005.02.007 (2005).
11. Chen, C.S., Mrksich, M., Huang, S., Whitesides, G.M., Ingber, D.E. Geometric Control of Cell Life and Death. *Science*. **276** (5317), 1425–1428, doi: 10.1126/science.276.5317.1425 (1997).
12. Whitesides, G.M., Ostuni, E., Takayama, S., Jiang, X., Ingber, D.E. Soft Lithography in Biology and Biochemistry. *Annual Review of Biomedical Engineering*. **3**, 335–373, doi: 10.1146/annurev.bioeng.3.1.335 (2001).
13. Cirelli, R.A., Watson, G.P., Nalamasu, O. Encyclopedia of Materials: Science and Technology. *Techniques and Processing: Surface, Micro-, and Nanoscale Processing*. 6441–6448, doi: 10.1016/b0-08-043152-6/01138-4 (2001).
14. Stricker, J., Aratyn-Schaus, Y., Oakes, P.W., Gardel, M.L. Spatiotemporal Constraints on the Force-Dependent Growth of Focal Adhesions. *Biophysical Journal*. **100** (12), 2883–2893, doi: 10.1016/j.bpj.2011.05.023 (2011).
15. Azioune, A., Storch, M., Bornens, M., Théry, M., Piel, M. Simple and rapid process for single cell micro-patterning. *Lab on a Chip*. **9** (11), 1640–1642, doi: 10.1039/b821581m (2009).
16. Chang, F., Atilgan, E., Burgess, D., Minc, N. Manipulating Cell Shape by Placing Cells into

- Microfabricated Chambers. *Methods in Molecular Biology*. **1136**, 281–290, doi: 10.1007/978-1-4939-0329-0_13 (2014).
17. Takeuchi, S., DiLuzio, W.R., Weibel, D.B., Whitesides, G.M. Controlling the Shape of Filamentous Cells of Escherichia Coli. *Nano Letters*. **5** (9), 1819–1823, doi: 10.1021/nl0507360 (2005).
18. Minc, N., Boudaoud, A., Chang, F. Mechanical Forces of Fission Yeast Growth. *Current Biology*. **19** (13), 1096–1101, doi: 10.1016/j.cub.2009.05.031 (2009).
19. Durand-Smet, P., Spelman, T.A., Meyerowitz, E.M., Jönsson, H. Cytoskeletal organization in isolated plant cells under geometry control. *Proceedings of the National Academy of Sciences*. **117** (29), 17399–17408, doi: 10.1073/pnas.2003184117 (2020).
20. Haske, W. *et al.* 65 nm feature sizes using visible wavelength 3-D multiphoton lithography.pdf. *Optics Express*. **15** (6), 3426–3436, doi: 10.1364/oe.15.003426 (2007).
21. Song, J., Michas, C., Chen, C.S., White, A.E., Grinstaff, M.W. From Simple to Architecturally Complex Hydrogel Scaffolds for Cell and Tissue Engineering Applications: Opportunities Presented by Two-Photon Polymerization. *Advanced Healthcare Materials*. **9** (1), 1901217, doi: 10.1002/adhm.201901217 (2020).
22. Torgersen, J., Qin, X., Li, Z., Ovsiannikov, A., Liska, R., Stampfl, J. Hydrogels for Two-Photon Polymerization: A Toolbox for Mimicking the Extracellular Matrix. *Advanced Functional Materials*. **23** (36), 4542–4554, doi: 10.1002/adfm.201203880 (2013).
23. Doyle, A.D., Wang, F.W., Matsumoto, K., Yamada, K.M. One-dimensional topography underlies three-dimensional fibrillar cell migration. *The Journal of Cell Biology*. **184** (4), 481–490, doi: 10.1083/jcb.200810041 (2009).
24. Doyle, A.D. Generation of Micropatterned Substrates Using Micro Photopatterning. *Current Protocols in Cell Biology*. **45** (1), 10.15.1-10.15.35, doi: 10.1002/0471143030.cb1015s45 (2009).
25. Waterman-Storer, C.M. Microtubule/Organelle Motility Assays. *Current Protocols in Cell Biology*. **00** (1), 13.1.1-13.1.21, doi: 10.1002/0471143030.cb1301s00 (1998).
26. Inoué, S., Spring, K.R. *Video Microscopy: The Fundamentals*. doi: 10.1007/978-1-4615-5859-0_5. Springer US. (1997).
27. Schneider, I.C., Hays, C.K., Waterman, C.M. Epidermal Growth Factor-induced Contraction Regulates Paxillin Phosphorylation to Temporally Separate Traction Generation from De-adhesion. *Molecular Biology of the Cell*. **20** (13), 3155–3167, doi: 10.1091/mbc.e09-03-0219 (2009).
28. Helmchen, F., Denk, W. Deep tissue two-photon microscopy. *Nature Methods*. **2** (12), 932–940, doi: 10.1038/nmeth818 (2005).
29. Xing, J., Cao, Y., Yu, Y., Li, H., Song, Z., Yu, H. In Vitro Micropatterned Human Pluripotent Stem Cell Test (μ P-hPST) for Morphometric-Based Teratogen Screening. *Scientific Reports*. **7** (1), 8491, doi: 10.1038/s41598-017-09178-1 (2017).
30. Ankam, S., Teo, B.K., Kukumberg, M., Yim, E.K. High throughput screening to investigate the interaction of stem cells with their extracellular microenvironment. *Organogenesis*. **9** (3), 0–14, doi: 10.4161/org.25425 (2013).

TITLE:

Control of cell geometry through infrared laser assisted micropatterning

AUTHORS AND AFFILIATIONS:

Shuying Yang¹, Chen Tuo¹, Ernest Iu¹, Sergey V Plotnikov¹

¹Department of Cell and Systems Biology, University of Toronto, Ontario, Canada

Email addresses of authors:

Shuying Yang (rosiey.yang@mail.utoronto.ca)

Chen Tuo (chen.tuo@mail.utoronto.ca)

Ernest Iu (ernest.iu@mail.utoronto.ca)

Corresponding author:

Sergey V Plotnikov (sergey.plotnikov@utoronto.ca)

SUMMARY:

The protocol presented here enables automated fabrication of micropatterns that standardizes cell shape to study cytoskeletal structures within mammalian cells. This user-friendly technique can be set up with commercially available imaging systems and does not require specialized equipment inaccessible to standard cell biology laboratories.

ABSTRACT:

Micropatterning is an established technique in the cell biology community used to study connections between the morphology and function of cellular compartments while circumventing complications arising from natural cell-to-cell variations. To standardize cell shape, cells are either confined in 3D molds or controlled for adhesive geometry through adhesive islands. However, traditional micropatterning techniques based on photolithography and deep UV heavily depend on clean rooms or specialized equipment. Here we present an infrared laser assisted micropatterning technique (microphotopatterning) modified from Doyle et al. that can be conveniently set up with commercially available imaging systems ~~{Doyle.Yamada.2009,Doyle.Doyle.2009}~~. In this protocol, we use a Nikon A1R MP+ imaging system to generate micropatterns with micron precision through an infrared (IR) laser that ablates preset regions on poly-vinyl alcohol coated coverslips. We employ a custom script to enable automated pattern fabrication with high efficiency and accuracy in systems not equipped with a hardware autofocus. We show that this IR laser assisted micropatterning (microphotopatterning) protocol results in clear patterns to which cells attach exclusively and take on the desired shape. Furthermore, data from a large number of cells can be averaged due to the standardization of cell shape. Patterns generated with this protocol, combined with imaging and analysis, can be used for relatively high throughput screens to understand molecular players mediating the link between form and function.

INTRODUCTION:

Cell shape is a key determinant of fundamental biological processes such as tissue morphogenesis¹, cell migration², cell proliferation³, and gene expression⁴. Changes in cell shape are driven by an intricate balance between dynamic rearrangements of the cytoskeleton that deforms the plasma membrane and extrinsic factors such as external forces exerted on the cell and the geometry of cell-cell and cell-matrix adhesions⁵. Migrating mesenchymal cells, for instance, polymerize a dense actin network at the leading edge that pushes the plasma membrane forward and creates a wide lamellipodia⁶, while actomyosin contractility retracts the cell's narrow trailing edge to detach the cell from its current position^{7, 8}. Disrupting signaling events that give rise to such specialized cytoskeletal structures perturbs shape polarity and slows cell migration⁹. In addition, epithelial sheet bending during gastrulation requires actomyosin-based apical constriction that causes cells and their neighbors to become wedge-shaped¹⁰. Although these studies highlight the importance of cell shape, the inherent heterogeneity in cell shape has encumbered efforts to identify mechanisms that connect morphology to function.

To this end, numerous approaches to manipulate cell shape have been developed over the past three decades. These approaches achieve their goal by either constraining the cell with a three-dimensional mold or controlling cellular adhesion geometry through patterned deposition of extracellular matrix (ECM) proteins onto an antifouling surface, a technique termed micropatterning¹¹. Here we will review a number of techniques that have gained popularity throughout the years.

Originally pioneered as an approach for microelectronic applications, soft lithography-based microcontact printing¹² has unequivocally become a cult favorite. A master wafer is first fabricated by selectively exposing areas of a photoresist-coated silicon substrate to photoirradiation¹³, leaving behind a patterned surface. An elastomer, such as PDMS, is then poured onto the master wafer to generate a soft "stamp" that transfers ECM proteins to a desired substrate^{11, 14}. Once fabricated, a master wafer can be used to cast many PDMS stamps that give rise to highly reproducible micropatterns¹². However, the patterns cannot be readily adjusted on demand due to the lengthy photolithography process. This process also requires highly specified equipment and cleanrooms that are not typically available in Biology departments.

More recently, direct printing using deep UVs has been reported to circumvent limitations posed by traditional lithography-based approaches. Deep UV light is directed through a photomask to selective areas of a glass coverslip coated with poly-L-lysine-*grafted*-polyethylene glycol. Chemical groups exposed to deep UV are photoconverted without the use of photosensitive linkers to enable binding of ECM proteins¹⁵. The lack of photosensitive linkers enables patterned coverslips to remain stable at room temperature for over seven months¹⁵. This method avoids the use of cleanrooms and photolithography equipment and requires less specialized training. However, the requirement for photomasks still poses a substantial hurdle for experiments that require readily available changes in patterns.

In addition to methods that manipulate cell geometry through controlled deposition of ECM proteins on a 2D surface, other seek to control cell shape by confining cells in 3D microstructures. Many studies have adapted the soft lithography-based approach described

above to generate 3D, rather than 2D, PDMS chambers to investigate shape-dependent biological processes in embryos, bacteria, yeast and plants^{16–19}. Two-photon polymerization (2PP) has also taken the lead as a microfabrication technique that can create complex 3D hydrogel scaffolds with nanometer resolution²⁰. 2PP relies on the principles of two-photon adsorption, where two photons delivered in femtometer pulses are absorbed simultaneously by a molecule – photoinitiator in this case – that enables local polymerization of photopolymers²¹. This technique has been heavily employed to print 3D scaffolds that mimic the native ECM structures of human tissue and has been shown to induce low photochemical damage to cells²².

The debut of microphotopatterning 10 years ago gave researchers the opportunity to fabricate micropatterns while avoiding inaccessible and specialized equipment. Microphotopatterning creates patterns on the micron scale by thermally removing selective regions of poly-vinyl alcohol (PVA) coated on activated glass surfaces using an infrared (IR) laser^{23, 24}. ECM proteins that attach only the underlying glass surface and not PVA then serve as biochemical cues to enable controlled spreading dynamics and cell shape. This method also offers superior flexibility since patterns can be readily changed in real time. Here, we provide a step-by-step protocol of microphotopatterning by using a commercial multi-photon imaging system. The described protocol is designed for rapid and automated fabrication of large patterns. We demonstrated that these patterns efficiently control cell shape by constraining the geometry of cell-ECM adhesions. Finally, we demonstrate that the described patterning technique modulates the organization and dynamics of the actin cytoskeleton.

PROTOCOL:

1. Coverslip preprocessing

- 1.1. Prepare squeaky-clean coverslips as described in Waterman-Storer, 1998²⁵.
- 1.2. Prepare 1% (3-aminopropyl)trimethoxysilane (APTMS) solution and incubate the coverslips in the solution for 10 min with gentle agitation. Make sure that coverslips move freely in the solution.
- 1.3. Wash coverslips twice with dH₂O for 5 min each.
- 1.4. Prepare 0.5% glutaraldehyde (GA) solution and incubate the coverslips in the solution for 30 min on a shaker. For 25 coverslips, use 50 mL glutaraldehyde solution. Make sure that coverslips move freely in the solution.
- 1.5. Wash coverslips three times with dH₂O for 10 min each.
- 1.6. Spin dry coverslips for 30 s using a custom-built coverslip spinner. A detailed description of the coverslip spinner has been published²⁶ and is available online (<https://mullinslab.ucsf.edu/home-built-coverslip-drierspinner/>). Activated coverslips can be stored for up to one month at +4 °C in a box with dividers so that they stand apart from each other.

2. PVA coating

- 2.1. Mix PVA (98% hydrolyzed PVA, MW 98000) with dH₂O to make a 5.6% solution.
- 2.2. Solubilize the mixture in a 90 °C water bath and immediately filter through a 0.2 µm filter in a biosafety cabinet while hot. Filter the stock solution again if it precipitates. PVA solution can be stored at room temperature for 3 months.
- 2.3. In a ~~Falcon~~ 15 mL tube, add one part HCl to eight parts PVA. Invert the tube carefully a few times to mix.
- 2.4. Pour 2 mL of the mixed solution into a 35mm petri dish and immerse/submerge a clean, preprocessed coverslip into the liquid, taking care that the coverslips do not stick to the bottom. Incubate at room temperature for 5 min on a shaker.
- 2.5. Carefully remove the coverslips from the solution. Use the coverslip spinner to spin coat for 40 s. In the meantime, clean the tweezers. Transfer the coverslip to a box and dry at +4 °C overnight. PVA-coated coverslips can be stored at +4 °C for up to two weeks.

3. Configuring the Multiphoton Microscope

NOTE 1: The described protocol is tuned up to create cell adhesive micropatterns of desired shape and size on upright or inverted multi-photon imaging systems, especially the ones that are not equipped with a hardware autofocus. Thus, for every field of view (FOV), the patterning script ablates a small area to create a fiduciary marker on the coverslip, uses a software autofocus to focus the microscope on the coverslip surface, and ablates the desired pattern. Running this script in a loop for adjacent FOVs robustly creates a large array of micropatterns (5 x 5 mm or larger) that constrain cell shape and modulate the activity of intracellular biological processes.

NOTE 2: The described protocol was developed for Nikon A1R MP+ imaging system controlled by NIS-Elements software. If an imaging system from another vendor is used for patterning, the optical configurations and patterning script should be adjusted according to the manufacturer's instructions.

- 3.1. Turn on the microscope software. Ensure that the "Apo LWD 25X/1.10W DIC N2" objective is mounted on the microscope.
NOTE: The protocol described here is optimized for a 25x/1.1 NA water immersion objective, but other objectives can also be used for patterning. Readers should be aware that patterning with a high-magnification objective (e.g., 40x and 60x) takes longer time as it significantly decreases the number of patterns ablated in each FOV. Low magnification objectives can be used for patterning as long as they provide uniform illumination across the FOV and laser power sufficient to ablate the PVA layer.

3.2. In the “A1plus MP GUI” window, set the laser line to 750 nm.

3.3. Setting up the “Image” optical configuration

NOTE: NIS-Elements provides users with several tools (graphical interface, an acquisition workflow builder JOBS, optical configurations, and macros) to control the microscope hardware. In this protocol, most of the hardware control is achieved through various optical configurations as well as ND Acquisition and ND Stimulation modules.

3.3.1. In the “Calibration” tab, click on “New Optical Configuration”. Name the optical configuration “Image”. This is the baseline optical configuration that allows imaging of the coverslip through reflectance. Leave all other options as default and select the appropriate objective.

3.3.2. In the “A1plus MP GUI” window, click on the “Settings” button to configure the hardware settings under this optical configuration. Set the “Stimulation laser” to “IR stim”, place the beam splitter (BS 20/80) in the light path, set the “Scanner Unit” to “Galvano” and select the appropriate descanned detector.

3.3.3. In the “A1plus Compact GUI” window, select a scan size and dwell time that is sufficient to capture small features on the coverslip (1.1 msec and 1024 pixels on our system, respectively). Click on the “Normal” button so no line averaging or line integration is performed. Make sure the “Use IR laser” box is checked. Set up unidirectional scanning for simplicity.

NOTE: If scan speed is of concern, bidirectional scanning can be used.

3.3.4. In the same window, adjust laser power and detector sensitivity to obtain bright but not saturated image of the coverslip surface. Setting laser power to 3 – 5% of the maximum power and detector sensitivity (“HV” slider) to 15 V is a good starting point.

3.3.5. In the “A1plus Scan Area” window, set zoom to 1 to capture the entire FOV.

3.3.6. Save the optical configuration.

3.4. Setting up the “Print_Fudiciary_Marker” optical configuration

3.4.1. Duplicate the “Image” optical configuration and rename it “Print_Fudiciary_Marker”.

3.4.2. In the “A1plus Compact GUI” window, select the smallest scan size and dwell time (64 pixels and 80.2 msec on our system, respectively).

- 3.4.3. Since no imaging is required in this step, set detector sensitivity to 0 and increase laser power to 30%. Higher laser power will thermally remove the PVA layer on the coverslip in the desired regions.
- 3.4.4. In the “A1plus Scan Area” window, set “Zoom” to maximum (15.87 for our system) and place the scan area in the middle of the FOV.
- 3.4.5. In the “ND Acquisition” window, set up a Z-stack experiment. Set movement in the Z position to “Relative” and select the appropriate Z device. Set the step size to 2 μm and the stack depth to 10 μm above and below to account for any unevenness in the microscope stage or the PVA surface between adjacent FOVs.

3.5. Setting up the “Autofocus” optical configuration

- 3.5.1. Duplicate the “Image” optical configuration and rename it “Autofocus”.
- 3.5.2. In the “A1plus Scan Area” window, decrease the “Zoom” factor so the FOV is slightly larger than the fiduciary marker. This ensures that other small features on the coverslip will not interfere with autofocusing.
- 3.5.3. In the “Devices” menu, select “Autofocus Set Up”. Set the scan thickness to that of the Z-stack in the Z-stack experiment (see step 3.5.5). The microscope will scan through this range and find the best focal plane using the fiduciary marker. Leave the step size as default.

3.6. Setting up the “Load_ROI” optical configuration

- 3.6.1. Duplicate the “Image” optical configuration and rename it “Load_ROI”.
- 3.6.2. In the “A1plus Compact GUI” window, set scan size identical to that of the ROI mask. This optical configuration will be used to capture an image onto which the ROI mask will be loaded. We used 2048 pixels to achieve an optimal balance between resolution and speed.
NOTE: It is essential that this captured image is identical in size to the ROI mask.

3.7. Setting up the “Micropattern” optical configuration

- 3.7.1. Duplicate the “Print_Fiduciary_Marker” optical configuration and rename it “Micropattern”.
- 3.7.2. Set the “Zoom” factor to one.

- 3.7.3. In the “A1plus MP GUI” window, increase the stimulation laser power to ablate PVA and select an appropriate scan speed (40% and 32 sec/frame in our experiments, respectively).
- 3.7.4. In the “ND Stimulation” window, set up a ND stimulation experiment. Add a few phases to the “Time Schedule” and set each as “Stimulation”. Ensure stimulation area and duration are correct.
NOTE: The number of phases can be adjusted according to the thickness and smoothness of the PVA layer as well as the laser power used in this optical configuration.
- 3.7.5. In the same window, enable the the “StgMoveMainZ(-1.000,1)” function before each phase. This again accounts for any deviations in the Z-direction.
NOTE: The distance and direction in which the objective moves can be adjusted according to the thickness and smoothness of the PVA layer.

3.8. Setting up the “Label_Surface” optical configuration

- 3.8.1. Duplicate the “Print_Fudiciary_Marker” optical configuration and rename it “Label_Surface”.
- 3.8.2. In the “A1plus Compact GUI” window, increase laser power significantly and set Zoom to one. High laser power used here will physically damage the glass coverslip and produce a label visible to the naked eye. This aids in locating the patterns in further experiments.

4. Generating the ROI mask and Setting up the macro

4.1. Generating the ROI mask

- 4.1.1. Use Adobe Photoshop or other available software to generate a 2048 × 2048 RGB image. The image corresponds to a FOV under the microscope (*i.e.* 532.48 × 532.48 μm, 0.26 μm per pixel). The image should have a black (0, 0, 0) background.
NOTE: A number of commercial and free image editors can be used to generate ROI masks for laser assisted micropatterning. Although we use Adobe Photoshop to generate the masks, GIMP and ImageJ/Fiji are also available as alternative free option.
- 4.1.2. Draw 8 – 12 white (255,255,255) patterns on the black background. Pattern size varies depending on cell type (~200 pixels in diameter). Leave a 500 × 500 blank area in the center of the image for autofocus. Leave sufficient space between adjacent patterns (>200 pixels) and at the boarder of the FOV for

optimal ablation and cell attachment. Patterns presented in this protocol are available on Github (<https://github.com/PlotnikovLab/Micropatterning>).

4.2. Setting up the macro

4.2.1. Click on the “Macro” menu and select “New Macro”.

4.2.2. Import the “Pattern_Stimulation” code available on Github (<https://github.com/PlotnikovLab/Micropatterning>) into the “New Macro” window. Save this piece of code to an appropriate folder.

4.2.3. Open another “New Macro” window and import the “Stage_Movement” code available on Github (<https://github.com/PlotnikovLab/Micropatterning>). Ensure that the “Stage_Movement” working directory in this code is identical to that in step 4.2.2. Save the “Stage_Movement” code to the same folder in step 4.2.2.

5. Generating micropatterns using photo ablation

5.1. Turn on the microscope and its accessories. Ensure that the IR laser has warmed up sufficiently prior to this.

5.2. Transfer the PVA-coated coverslip onto a holder. For an upright microscope, ensure the PVA surface to be ablated faces down.

5.3. Add water to the corners to stabilize the coverslip and mount the holder onto the microscope stage.

5.4. Lower the objective and add water onto the coverslip.

NOTE: The protocol described here is optimized for a 25x/1.1 NA water immersion objective. If a dry or oil immersion objective is used, water should be replaced with an appropriate immersion media. When a water immersion objective is used to generate a large micropattern array, evaporation might become an issue. If this is the case, water should be replaced with GenTeal, an over-the-counter eye lubricant available from pharmacies.

5.5. In the microscope software, turn on the IR laser shutter in the “A1plus MP GUI” window. Click on the “Autoalignment” button to align the laser prior to patterning.

NOTE: It is crucial to perform laser autoalignment at the beginning of each patterning session as small deviations in the laser path will significantly affect the quality of the patterns.

5.6. Switch to the “Image” optical configuration. In the “A1plus Compact GUI” window, click “Scan” to scan the FOV while slowly moving the objective closer to the coverslip.

- 5.7. Carefully monitor the image. At first, the image will appear extremely dim. Move the objective closer to the coverslip until the image brightness increases. This is the coverslip surface that is facing the objective. Continue to move the objective until the brightness decreases and increases again. This is the PVA surface to be patterned. Focus on any small feature (coverslip imperfections, dust, etc.) on this surface and set zero on the Z drive. Always set zero after focusing.
NOTE: Although both surfaces of the coverslip are coated with PVA, the optical properties are not significantly altered. We routinely image such coverslips with dry, water- and oil-immersion objectives and did not find the non-patterned PVA surface to interfere with imaging.
- 5.8. Switch to the "Label_Surface" optical configuration. Click on "Capture". Return to "Imaging" and scan. The glass surface should be damaged and appear amorphous. The damaged area is visible to the naked eye, indicating the location of patterns in further experiments.
NOTE: To increase the size of the visible label, repeat step 5.8 in multiple adjacent FOVs.
- 5.9. Check again that the objective is roughly in the center of the coverslip. Ensure that there is sufficient water between the objective and the coverslip. Move the stage by 1 to 2 FOVs to avoid glass particles and scan to confirm.
- 5.10. In the "Devices" menu, open the "Stage_Movement" macro. Check that the "Pattern_Stimulation" working directory is correct; if not, stimulation will not occur. Set the variables "m" and "n" to the desired number of FOVs that will be patterned. Save and run the macro.
- 5.11. After patterning is complete, switch to the "Imaging" optical configuration. Again, check that the IR laser shutter is open in the "A1plus MP GUI" window.
- 5.12. Move the stage to view the patterns. Scan through the patterns to check their quality.
- 5.13. Transfer the coverslip to the grid box, with patterns facing up.
- 5.14. Store patterned coverslips at +4 °C for up to one week before use.

6. Fibronectin adsorption

- 6.1. Make fresh 1M NaBH₄ in 1M NaOH solution. Add at a 1:100 ratio to pH 8.0 phosphate buffer containing 0.2M ethanolamine.
- 6.2. Transfer patterned coverslips to a 35 mm tissue culture dish. Incubate each coverslip with 1 mL of the solution above for 8 min to quench autofluorescence, then rinse 3 times with PBS.

- 6.3. Dilute fibronectin (FN) in PBS to a final concentration of 10 µg/mL. Incubate the coverslip in FN for 1 h at +37 °C.

NOTE: If substantial nonspecific binding of ECM protein to the substrate is observed, FN can be diluted in PBS containing 0.1% Pluronic F-127²⁴.

- 6.4. Wash the coverslip 2 times with PBS. If not immediately used, store in PBS at +4 °C overnight.

7. Cell attachment

NOTE: The following protocol is optimized for primary human gingival fibroblasts.

- 7.1. Culture a 10 cm dish of cells to 70% confluency.
- 7.2. Warm up cell culture media, PBS and 0.05% trypsin in a +37 °C water bath.
NOTE: For cells that adhere weakly to the substrate, non-proteolytic dissociation with versene (0.48 mM EDTA) or a proprietary enzyme-free buffer may increase cell attachment to the patterns and should be considered.
- 7.3. Prior to seeding cells, relocate the patterned coverslip to a clean 35 mm tissue culture dish containing 1 mL warm PBS.
- 7.4. Aspirate the cell culture media from the 10cm tissue culture dish and wash once with PBS.
- 7.5. Add 700 µL of 0.05% trypsin/EDTA to the dish and incubate cells in a +37 °C, 5% CO₂ incubator for 1 min.
- 7.6. In the meantime, aspirate the PBS covering the patterned coverslip and add 1 mL of cell culture media.

Confirm that cells have detached, then resuspend the trypsinized cells with 10 mL of cell culture media and add 1 mL to the patterned coverslip.

- 7.7. Culture cells in the incubator for 2 – 3 h and check if a sufficient number of cells have attached to the patterns. If so, change media once to remove unattached cells. This minimizes the chance of multiple cells landing on the same pattern.
NOTE: Attachment time may vary depending on cell type.
- 7.8. After another 3-4 h, or when a sufficient number of cells have spread on patterns, cells are ready for further experiments. Do not wait for too long to avoid cell division.

8. Data acquisition

- 8.1. Fix cells with 4% PFA in cytoskeleton buffer²⁷ for 10 min at room temperature.
- 8.2. Follow immunofluorescence protocols established for the proteins of interest. PVA-coated coverslips work well with any immunofluorescence protocol.
- 8.3. Acquire images of cells using an appropriate microscope. Depending on the goal of the experiment, you may image either one or multiple cells per FOV.

9. Image analysis

NOTE: The following protocol allows users to obtain the average fluorescence signal of the protein of interest over a large number of cells from Z-stacks of microscope images.

- 9.1. Open the acquired images in NIS Elements and crop the images. Ensure that each image contains only one well-spread cell. Detailed instructions on image processing can be found in the script below.
- 9.2. Install Anaconda and launch Spyder through Anaconda Navigator.
NOTE: The .py scripts can be run in any environment with the appropriate packages identified in the requirements.txt file installed. We recommend Anaconda because it contains most of the required packages for the codes below.
- 9.3. Download the script from Github (<https://github.com/PlotnikovLab/Micropatterning>) and open in Spyder (“Pattern_Averaging_3Channels.py” or “Pattern_Averaging_4Channels.py” for images with 3 Channels or 4 Channels, respectively).
- 9.4. Set parameters based on the acquired images. See the script for detailed descriptions.
- 9.5. Press F5 to run the script. The progress can be tracked in the Console panel.
- 9.6. Retrieve the output files saved in the same folder. The output images are the average of each channel for all samples. The excel sheet shows the mean intensity of each channel within a sample cell, which enables further quantitative analysis.

REPRESENTATIVE RESULTS:

The quality of the experimental data obtained with a micropatterning technique is largely dependent on the quality of the patterns. To determine the quality of patterns generated with the method above, we first used reflectance microscopy to assess the shape and size of the photo ablated areas of the coverslip. We found that each individual pattern looked very similar to the ablation mask and displayed clear borders and a surface that reflected light uniformly (**Fig 2B**). A variety of shapes and sizes can be printed depending on the desired cytoskeleton architecture, but we used the crossbow shape that best suits our purposes. Atomic force microscopy (AFM) revealed that such patterns were approximately 140 nm in height and had a smooth surface with

minimal topological variation throughout (**Fig 2F**). Suboptimal patterning settings, such as low laser power and incorrect focal plane, resulted in incomplete removal of the PVA surface that manifests as darker, partial patterns with uneven topology (**Fig 2C**). Setting laser power too high resulted in PVA “bubbling” and when extreme, coverslip surface damage that is also undesirable (**Fig 2D**).

In preliminary experiments we attempted to increase the patterning area by abating multiple FOVs on a single coverslip. We found that this approach, although works in principle, is unreliable and tedious due to Z-drift of the microscope stand and slight tilt of the coverslip. To achieve high-quality patterns over a large number of FOVs in an automated fashion, we implemented a customized macro that improved the precision of microscope focusing during the patterning process. The multiphoton microscope employs a pulse laser that efficiently degrades PVA with high power in a narrow focal plane, making the patterning process sensitive to any unevenness or tilt in the sample. As a result, it is important to identify the precise focal plane in each FOV. This is even more problematic for systems lacking a perfect focus module, as deviations as little as one to two microns can render the patterning process fruitless. To address this problem, the customized macro script first patterns a small square in the center of each new FOV that is only roughly in focus by scanning through a relatively thick Z-stack ($\approx 20\ \mu\text{m}$). The microscope then quickly scans through the stack of images and uses NIS Elements autofocus function to identify the optimal focal plane. The pattern mask is then loaded and set as stimulation ROI for IR stimulation to occur. The stage subsequently moves to the next FOV and repeats this process. In addition, the square-wave shaped path of the microscope stage movement ensured minimal error accumulation between sequential FOVs. By using this protocol, we routinely fabricate patterns composed of 49 microscope FOVs covering $3.5 \times 3.5\ \text{mm}$ area of the coverslip in less than 3 hrs.

To test if patterned areas, not unperturbed PVA, could adsorb ECM proteins, we coated patterned coverslips with $10\ \mu\text{g/mL}$ FN and stained them with anti-FN antibody. Using wide field fluorescent microscopy, we found that FN uniformly adsorbed to the patterned areas where PVA had been removed by laser degradation (**Fig 2E**).

To determine if cytoskeleton architecture and tension distribution could be modified as expected on the patterns, we seeded cells on patterned coverslips and visualized the distribution of myosin light chain, a marker of contractility, through fluorescence microscopy. After initial seeding, cells gradually gravitated towards the coverslip. Those that landed on patterned areas attached and spread into the shape of the pattern over time. Those that landed on PVA only loosely attached and were removed after several washes and media changes. We found that cells spread on patterns displayed phenotypical fibroblast structures including an actin-dense rim of lamellipodia, thick ventral stress fibers along the two sides, and dorsal stress fibers emanating from the lamellipodia connected by transverse arcs (**Fig 3A**). Myosin light chain (MLC) sat behind the dense lamellipodia rim and displayed a striated pattern along actin bundles. As indicated by averaged images of many cells, this phenotype was consistent across a large number of patterns (**Fig 3B**).

FIGURE AND TABLE LEGENDS:

Figure 1. Schematic of IR laser assisted micropatterning (microphotopatterning). (A) Glass coverslips are chemically coated with APTMS, GA and PVA, in the respective order. The PVA surface is non-adhesive to cells and proteins. (B) PVA is removed in preset patterns by an IR laser. (C) Patterned coverslips are coated with ECM protein that will only adsorb to patterned areas. (D) Cells are plated on coverslips, fixed, and immunostained for proteins of interest. Cells that land on patterned islands spread into the shape of the pattern that gives rise to characteristic cytoskeletal structures, while those that land on PVA remain spherical.

Figure 2. Micropattern validation and characterization. (A) IR laser assisted micropatterning (microphotopatterning) setup on a microscope stage. The IR laser thermally ablates PVA in multiple FOVs. (B) A reflectance microscopy image of micropatterns that have clear borders and are identical to the ROI masks. (C) A reflectance microscopy image of incomplete removal of PVA resulting from suboptimal laser power. (D) A reflectance microscopy image of PVA bubbling and (corners) and coverslip surface damage resulting from excess laser power. (E) Immunofluorescence images of FN coated patterned coverslips stained with anti-FN primary antibodies and fluorophore-conjugated secondary antibodies. (F) An AFM topology scan line and a representative AFM image of a crossbow pattern. To measure the topology of the micropattern, contact mode imaging was performed using a Bruker AFM probe (MLCT-B) mounted on a NanoWizard 4 atomic force microscope.

Figure 3. Representative images of cells plated on micropatterns. (A) Representative images of a primary human gingival fibroblast plated on crossbow patterns immunostained for actin and MLC. Images were acquired with a confocal microscope and a 100X objective. (B) Averaged immunofluorescence images of actin and MLC in cells plated on crossbow patterns generated by a custom Python script.

DISCUSSION:

The results above demonstrate that the described IR laser assisted micropatterning (microphotopatterning) protocol provides reproducible adherent patterns of various shapes that enables the manipulation of cell shape and cytoskeletal architecture. Although numerous micropatterning methods have been described both prior to and after the debut of microphotopatterning, this method possesses several advantages. First, it does not require specialized equipment and cleanrooms that are usually only found within Engineering departments. In fact, as multiphoton microscopes are becoming a more common sight in Biology departments, microphotopatterning expands the applications of the multiphoton microscope and adds to the potential pool of users. Patterns can also be changed on demand with commercially available software, such as Photoshop and ImageJ, and printed immediately, instead of having to fabricate a new master wafer that entails a lengthy lithography process.

Compared to the pre-existing microphotopatterning protocol, one improvement in our protocol is the elimination of several time-consuming curing steps during coverslip preparation. We show that the quality of PVA-coverslip attachment remains unperturbed as the patterns were still intact and could bind cells even two weeks after fabrication. More importantly, we improved

automation of the patterning process by eliminating the need to preset the position of each FOV²⁴. Instead, we implement an understandable macro that allows patterning of a large area while precisely identifying the optimal focal plane of each FOV.

Although the macros in our protocol enable automation of patterning on our system, we understand that every commercial laser scanning microscope comes with their own proprietary software that is rarely compatible with others, making it difficult to implement our exact protocol on other systems. However, the overall workflow can be well adapted to other commercial systems to facilitate automated micropatterning, namely the process of focusing on each individual FOV, loading the mask, ablating PVA, and moving the microscope stage to a new FOV.

Several steps in our patterning protocol should be undertaken with great care to ensure efficient patterning. The most critical step is to optimize stimulation conditions before generating patterns. In multi-photon microscopy, two or more photons must arrive almost simultaneously at a fluorescent molecule and combine their energy to excite fluorescence. This low probability event creates an extremely thin optical section that increases signal-to-noise ratio²⁸. Although beneficial for imaging, this feature makes the removal of the thin PVA coating extremely sensitive to the sample's Z-position. Several measures can be implemented to counter this. First, laser power should be fine-tuned to ensure thorough removal of PVA without "boiling" the polymer or damaging the glass coverslip. If PVA removal is consistently incomplete, we recommend checking laser alignment as this usually increases laser power. Second, the microscope stage should be leveled to avoid sample tilt, which could result in incomplete patterns. IR stimulations in multiple Z-positions should also be set up to ensure that the PVA layer is targeted. Alternatively, if the microscope is equipped with a perfect focus module, preliminary tests can be conducted to determine the optimal offset in Z-position for PVA targeting. Another critical step is to set up a microscope macro that allows pattern stimulation in an automated fashion. The macro should find the focal plane of each new FOV to avoid complications from sample tilt or surface unevenness. It should also allow the stage to move in an S-shape from row to row, analogous to the path taken in bi-directional scanning, to minimize deviations in Z between consecutive FOVs.

One limitation to the protocol described is the time required to produce a large number of patterned coverslips, an unparalleled advantage offered by lithography-based microcontact printing^{29, 30}. As a result, this protocol is best suited for experiments in which a limited number of conditions are required, or those that require readily available adjustments in pattern shape and size. Furthermore, for systems lacking a hardware autofocus module, we integrate a series of stimulation events in different z-planes to ensure automated and effective PVA removal. Since IR stimulation is the most time-consuming step, the addition of each stimulation event (~30 sec) significantly lengthens the patterning process. If time is of concern, we suggest fine tuning autofocus by decreasing step size. This facilitates the identification of the best focal plane which will decrease the number of IR stimulation events required. In our experiments, decreasing the number of stimulation events from five to two reduces the time by half (1.5 h).

In conclusion, the IR laser assisted micropatterning (microphotopatterning) protocol we describe can be used in any lab that has access to an IR laser-equipped microscope. In addition

to studying cytoskeletal architecture and signaling pathways that connect form to function, this technique can also be applied to drug screening and other applications that are sensitive to cell-to-cell variability.

ACKNOWLEDGMENTS: This work was supported by Connaught Fund New Investigator Award to S.P., Canada Foundation for Innovation, NSERC Discovery Grant Program (grants RGPIN-2015-05114 and RGPIN-2020-05881), University of Manchester and University of Toronto Joint Research Fund, and University of Toronto XSeed Program. C.T. was supported by NSERC USRA fellowship.

DISCLOSURES:

The authors disclose no conflict of interests.

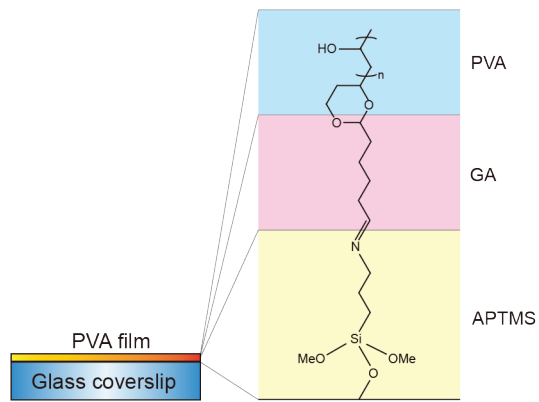
REFERENCES:

1. Harris, T.J.C., Sawyer, J.K., Peifer, M. How the Cytoskeleton Helps Build the Embryonic Body Plan Models of Morphogenesis from Drosophila. *Current Topics in Developmental Biology*. **89**, 55–85, doi: 10.1016/s0070-2153(09)89003-0 (2009).
2. Keren, K. *et al.* Mechanism of shape determination in motile cells. *Nature*. **453** (7194), 475–480, doi: 10.1038/nature06952 (2008).
3. Castor, L.N. Control of Division by Cell Contact and Serum Concentration in Cultures of 3T3 Cells. *Experimental Cell Research*. **68** (1), 17–24, doi: 10.1016/0014-4827(71)90581-7 (1971).
4. Jain, N., Iyer, K.V., Kumar, A., Shivashankar, G.V. Cell geometric constraints induce modular gene-expression patterns via redistribution of HDAC3 regulated by actomyosin contractility. *Proceedings of the National Academy of Sciences*. **110** (28), 11349–11354, doi: 10.1073/pnas.1300801110 (2013).
5. Paluch, E., Heisenberg, C.-P. Biology and Physics of Cell Shape Changes in Development. *Current Biology*. **19** (17), R790–R799, doi: 10.1016/j.cub.2009.07.029 (2009).
6. Pollard, T.D., Borisy, G.G. Cellular Motility Driven by Assembly and Disassembly of Actin Filaments. *Cell*. **112** (4), 453–465, doi: 10.1016/s0092-8674(03)00120-x (2003).
7. Ridley, A.J. *et al.* Cell Migration: Integrating Signals from Front to Back. *Science*. **302** (5651), 1704–1709, doi: 10.1126/science.1092053 (2003).
8. Cramer, L.P. Mechanism of cell rear retraction in migrating cells. *Current Opinion in Cell Biology*. **25** (5), 591–599, doi: 10.1016/j.ceb.2013.05.001 (2013).
9. Lee, J., Ishihara, A., Oxford, G., Johnson, B., Jacobson, K. Regulation of cell movement is mediated by stretch-activated calcium channels. *Nature*. **400** (6742), 382–386, doi: 10.1038/22578 (1999).
10. Leptin, M. Gastrulation Movements: the Logic and the Nuts and Bolts. *Developmental Cell*. **8** (3), 305–320, doi: 10.1016/j.devcel.2005.02.007 (2005).
11. Chen, C.S., Mrksich, M., Huang, S., Whitesides, G.M., Ingber, D.E. Geometric Control of Cell Life and Death. *Science*. **276** (5317), 1425–1428, doi: 10.1126/science.276.5317.1425 (1997).
12. Whitesides, G.M., Ostuni, E., Takayama, S., Jiang, X., Ingber, D.E. Soft Lithography in Biology and Biochemistry. *Annual Review of Biomedical Engineering*. **3**, 335–373, doi:

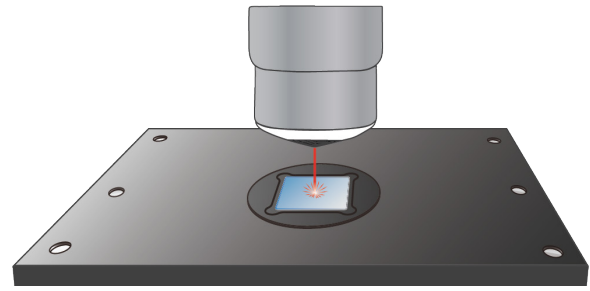
- 10.1146/annurev.bioeng.3.1.335 (2001).
13. Cirelli, R.A., Watson, G.P., Nalamasu, O. Encyclopedia of Materials: Science and Technology. *Techniques and Processing: Surface, Micro-, and Nanoscale Processing*. 6441–6448, doi: 10.1016/b0-08-043152-6/01138-4 (2001).
14. Stricker, J., Aratyn-Schaus, Y., Oakes, P.W., Gardel, M.L. Spatiotemporal Constraints on the Force-Dependent Growth of Focal Adhesions. *Biophysical Journal*. **100** (12), 2883–2893, doi: 10.1016/j.bpj.2011.05.023 (2011).
15. Azioune, A., Storch, M., Bornens, M., Théry, M., Piel, M. Simple and rapid process for single cell micro-patterning. *Lab on a Chip*. **9** (11), 1640–1642, doi: 10.1039/b821581m (2009).
16. Chang, F., Atilgan, E., Burgess, D., Minc, N. Manipulating Cell Shape by Placing Cells into Microfabricated Chambers. *Methods in Molecular Biology*. **1136**, 281–290, doi: 10.1007/978-1-4939-0329-0_13 (2014).
17. Takeuchi, S., DiLuzio, W.R., Weibel, D.B., Whitesides, G.M. Controlling the Shape of Filamentous Cells of Escherichia Coli. *Nano Letters*. **5** (9), 1819–1823, doi: 10.1021/nl0507360 (2005).
18. Minc, N., Boudaoud, A., Chang, F. Mechanical Forces of Fission Yeast Growth. *Current Biology*. **19** (13), 1096–1101, doi: 10.1016/j.cub.2009.05.031 (2009).
19. Durand-Smet, P., Spelman, T.A., Meyerowitz, E.M., Jönsson, H. Cytoskeletal organization in isolated plant cells under geometry control. *Proceedings of the National Academy of Sciences*. **117** (29), 17399–17408, doi: 10.1073/pnas.2003184117 (2020).
20. Haske, W. *et al.* 65 nm feature sizes using visible wavelength 3-D multiphoton lithography.pdf. *Optics Express*. **15** (6), 3426–3436, doi: 10.1364/oe.15.003426 (2007).
21. Song, J., Michas, C., Chen, C.S., White, A.E., Grinstaff, M.W. From Simple to Architecturally Complex Hydrogel Scaffolds for Cell and Tissue Engineering Applications: Opportunities Presented by Two-Photon Polymerization. *Advanced Healthcare Materials*. **9** (1), 1901217, doi: 10.1002/adhm.201901217 (2020).
22. Torgersen, J., Qin, X., Li, Z., Ovsianikov, A., Liska, R., Stampfl, J. Hydrogels for Two-Photon Polymerization: A Toolbox for Mimicking the Extracellular Matrix. *Advanced Functional Materials*. **23** (36), 4542–4554, doi: 10.1002/adfm.201203880 (2013).
23. Doyle, A.D., Wang, F.W., Matsumoto, K., Yamada, K.M. One-dimensional topography underlies three-dimensional fibrillar cell migration. *The Journal of Cell Biology*. **184** (4), 481–490, doi: 10.1083/jcb.200810041 (2009).
24. Doyle, A.D. Generation of Micropatterned Substrates Using Micro Photopatterning. *Current Protocols in Cell Biology*. **45** (1), 10.15.1-10.15.35, doi: 10.1002/0471143030.cb1015s45 (2009).
25. Waterman-Storer, C.M. Microtubule/Organelle Motility Assays. *Current Protocols in Cell Biology*. **00** (1), 13.1.1-13.1.21, doi: 10.1002/0471143030.cb1301s00 (1998).
26. Inoué, S., Spring, K.R. *Video Microscopy: The Fundamentals*. doi: 10.1007/978-1-4615-5859-0_5. Springer US. (1997).
27. Schneider, I.C., Hays, C.K., Waterman, C.M. Epidermal Growth Factor-induced Contraction Regulates Paxillin Phosphorylation to Temporally Separate Traction Generation from De-adhesion. *Molecular Biology of the Cell*. **20** (13), 3155–3167, doi: 10.1091/mbc.e09-03-0219 (2009).
28. Helmchen, F., Denk, W. Deep tissue two-photon microscopy. *Nature Methods*. **2** (12), 932–940, doi: 10.1038/nmeth818 (2005).

29. Xing, J., Cao, Y., Yu, Y., Li, H., Song, Z., Yu, H. In Vitro Micropatterned Human Pluripotent Stem Cell Test (μ P-hPST) for Morphometric-Based Teratogen Screening. *Scientific Reports*. **7** (1), 8491, doi: 10.1038/s41598-017-09178-1 (2017).
30. Ankam, S., Teo, B.K., Kukumberg, M., Yim, E.K. High throughput screening to investigate the interaction of stem cells with their extracellular microenvironment. *Organogenesis*. **9** (3), 0–14, doi: 10.4161/org.25425 (2013).

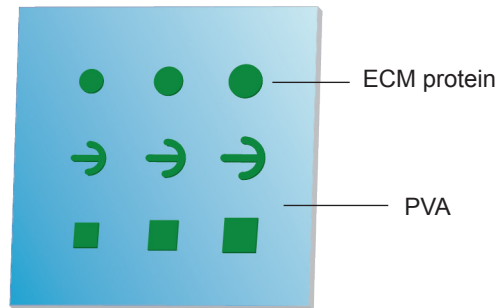
A



B

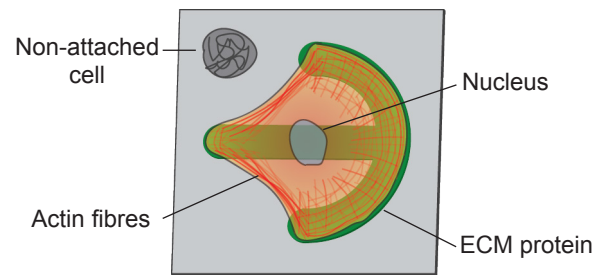


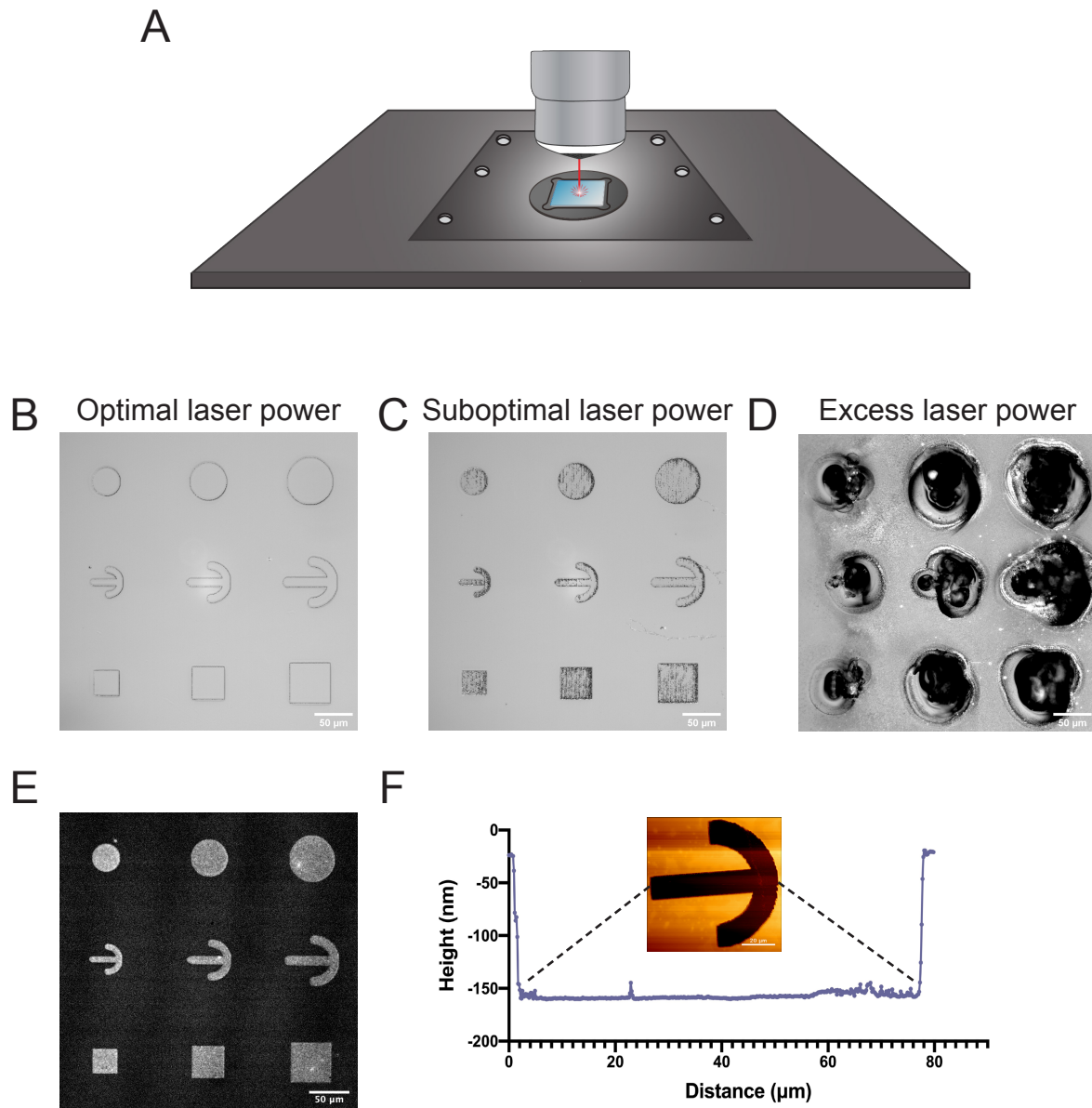
C

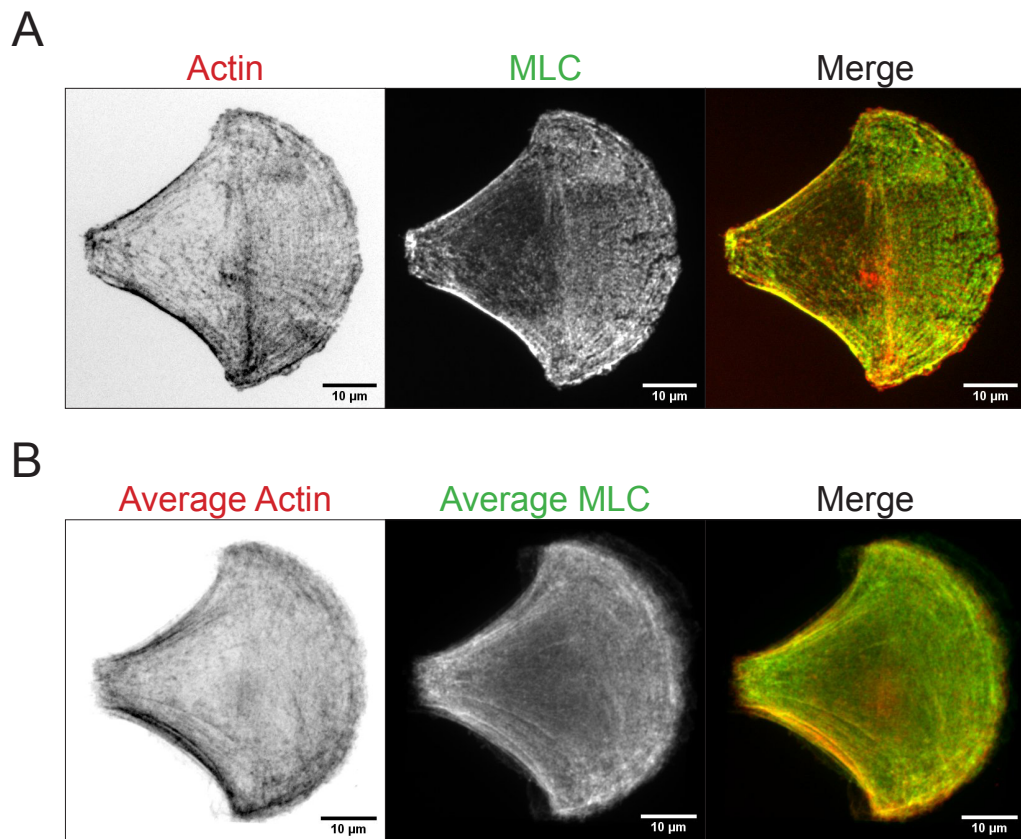


One field of view (532.48 μm)

D







| Name | Company | Catalog Number |
|--------------------------------------|------------------------------|------------------|
| (3-Aminopropyl)trimethoxysilane | Aldrich | 281778 |
| 10 cm Cell Culture Dish | VWR | 10062-880 |
| 25X Apo LWD Water Dipping Objective | Nikon | MRD77225 |
| 3.5 cm Cell Culture Dish | VWR | 10861-586 |
| 4',6-Diamidino-2-Phenylindole (DAPI) | Thermo | 62248 |
| Bovine Serine Albumin | BioShop | ALB005 |
| Dulbecco's Phosphate-Buffered Saline | Wisent | 311-425-CL |
| Ethanolamine | Sigma-Aldrich | E9508 |
| Fibronectin | Sigma-Aldrich | FC010 |
| Fibronectin Antibody | BD | 610077 |
| Fiji | ImageJ | |
| Fluorescent Phalloidin | Invitrogen | A12380 |
| Glass Coverslip | VWR | 16004-302 |
| Glutaraldehyde | Electron Microscopy Sciences | 16220 |
| Hydrochloric Acid | Caledon | 6025-1-29 |
| IR Laser | Coherent | Chameleon Vision |
| Minimal Essential Medium α | Gibco | 12561-056 |
| Mounting Medium | Sigma | F4680 |
| Mouse Secondary Antibody | Cell Signaling Technology | 4408S |
| Multi-Photon Microscope | Nikon | A1R MP+ |
| Myosin Light Chain Antibody | Cell Signaling Technology | 3672S |
| NIS Elements | Nikon | |
| Nitric Acid | Caledon | 7525-1-29 |
| Photoshop | Adobe | |
| Pluronic F-127 | Sigma | P2443 |
| Poly(vinyl alcohol) | Aldrich | 341584 |
| Rabbit Secondary Antibody | Cell Signaling Technology | 4412S |
| Shaker | VWR | 10127-876 |
| Sodium Borohydride | Aldrich | 452882 |
| Sodium Hydroxide | Sigma-Aldrich | S8045 |
| Sodium Phosphate Dibasic | Sigma | S5136 |
| Sodium Phosphate Monobasic | Sigma | S5011 |
| Spyder | Anaconda | 4.1.4 |
| Trypsin | Wisent | 325-042-CL |

Comments

Polystyrene, TC treated, vented

Polystyrene, TC treated, vented
1mg/mL dihydrochloride solution

1mg/mL in pH 7.5 buffer

Mouse

Version 1.53c

568nm

22 × 22 mm

25% aqueous solution

37% aqueous solution

Goat, 488nm

Rabbit

Version 5.21.03

70% aqueous solution

Version 21.2.1

Powder

MW 89000-98000, 98% hydrolyzed

Goat, 488nm

Also known as analog rocker

Powder

Powder

Powder

0.05% aqueous solution with 0.53mM EDTA



Cell & Systems Biology
UNIVERSITY OF TORONTO

April 5th, 2021

Dear Dr Myers,

We are hereby re-submitting our manuscript entitled “Control of cell geometry through laser assisted micropatterning” (manuscript number: JoVE62492) to JoVE. We appreciate the consideration of the paper and the reviewers’ helpful suggestions and insightful criticisms. We are encouraged by the positive comments and have worked hard to address the major concerns in the revised manuscript. We truly believe that the changes inspired by the reviewers have made the manuscripts substantially better. In this letter, we provide a brief summary of the revisions made to the original manuscript as well as detailed point-by-point responses to the reviewers’ comments.

As per the editor’s comments and suggestions, we carefully proofread the manuscript to ensure a logical and comprehensible flow between statements. Additionally, the protocol was thoroughly revised to further parallel the spoken directions within the video, homogenizing the video and manuscript. Only a select few directions and notes were verbally omitted from the video as they are visually demonstrated. Furthermore, all sound edits and visual suggestions were successfully integrated.

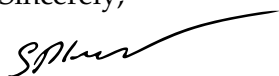
To address the reviewers’ concern of a narrow range of imaging system that are compatible with our protocol, we included a note section with a detailed description of how the overall workflow described in the protocol can be reproduced on a multi-photon microscope from a different vendor. We also provided several lines of evidence to convince the reviewers that our protocol is fully compatible with any multi-photon imaging system controlled by NIS Elements and will retain the compatibility for the foreseeable future.

We revised the macros and Python scripts provided with this protocol to make them more interactive and user friendly. In accordance with the reviewers’ suggestions, we revised the Python scripts to ensure their compatibility with various computer platforms and operating systems. The updated scripts work correctly on Windows 10 and MacOS.

Additionally, we refined the text of the manuscript according to the reviewers’ suggestions. We revised the manuscript with the intention of avoiding any overinterpretations and misleading statements, which were present in the initial submission, and to clarify and unclutter the protocol. We hope we have achieved these goals. We also slightly expanded the Introduction section to provide a more comprehensive review of published micropatterning techniques.

We are immensely grateful for the reviewers and their comments, and we hope that our detailed point-by-point responses provided below alleviate reviewer’s concerns and make the manuscript acceptable for publication in JoVE.

Sincerely,



Sergey V Plotnikov, PhD
Assistant Professor

Detailed responses to the reviewer's comments and questions

Reviewer 1:

1.6 The link on proweb.org is dead.

We apologize for the dead link for the coverslip spinner description. The link in the revised manuscript was updated as follows (page 4):

"1.6 Spin dry coverslips for 30 s using a custom-built coverslip spinner. A detailed description of the coverslip spinner has been published{Inoué.Spring.1997} and is available online (<https://mullinslab.ucsf.edu/home-built-coverslip-drierspinner/>). Activated coverslips can be stored for up to one month at +4 °C in a box with dividers so that they stand apart from each other."

4.1.1 use GIMP or ImageJ or Photoshop.

We agree with the reviewer that commercial image editors are not essential for generating the ROI masks. The following Note was included in the manuscript to elaborate on the available free options (page 7):

"4.4.1. NOTE: A number of commercial and free image editors can be used to generate ROI masks for laser assisted micropatterning. Although we use Adobe Photoshop to generate the masks, GIMP and ImageJ/Fiji are also available as alternative free option."

5.3 why is the water needed? How is it possible to have water on an inverted microscope?

The requirement to add water or other immersion media is strictly determined by the objective used for micropatterning. We optimized the protocol for 25x/1.1NA water immersion objective, but dry and oil-immersion objectives with an appropriate immersion media can also be used for micropatterning. We stated this in the following Note on page 8:

"NOTE: The protocol described here is optimized for 25x/1.1 NA water immersion objective. If a dry or oil-immersion objective is used for micropatterning, water should be replaced with an appropriate immersion media."

Water immersion objectives are routinely used on both upright and inverted imaging systems - surface tension of water is sufficient to hold it in place on the objective. But water evaporation can, in fact, be an issue for printing over a large coverslip area. Thus, we included the following statement in the Note on page 8:

"When water immersion objective is used to generate a large micropattern array, evaporation might become an issue. If this is the case, water should be replaced with GenTeal, an over-the-counter eye lubricant available from a pharmacy."

6.3 why is the pluronic needed here?

In our hands Pluronic is not essential for coating the micropatterns with ECM proteins. It has been reported that Pluronic decreases non-specific protein absorption to the patterned surface, but even in the absence of pluronic we did not observe cell attachment outside patterned islands. Thus, we revised the results section of the manuscript as follows (page 10):

"6.3. Dilute fibronectin (FN) in PBS to a final concentration of 10 µg/mL. Incubate the coverslip in FN for 1 h at +37 °C."

NOTE: *If substantial nonspecific binding of ECM protein to the substrate is observed, FN can be diluted in PBS containing 0.1% Pluronic F-127{Doyle.Doyle.2009}.*

7.2 should recommend EDTA/Versene instead of trypsin for easier reattachment.

As the reviewer suggested, we expanded the list of cell detachment techniques mentioned in Step 7.2. The following text was added on page 10:

“7.2 NOTE: For cells that adhere weakly to the substrate, non-proteolytic dissociation with versene (0.48 mM EDTA), or a proprietary enzyme-free buffer that may increase cell attachment to the patterns should be considered. “

9.2 Authors must not assume an Anaconda environment but must make the script runnable everywhere. See comments below

We appreciate the reviewer’s suggestion to improve code implementation in other environments. In accordance with the suggestions, we have added a requirements.txt file listing the required packages and have added instructions. For the purpose of this protocol, we recommend an Anaconda environment because it contains most packages that are required for the codes, with only a small number of packages requiring additional installation. We have added the following Note on page 11 for clarification:

“NOTE: The .py scripts can be run in any environment with the appropriate packages identified in the requirements.txt file installed. We recommend Anaconda because it contains most of the required packages for the codes below.”

In order to allow as many labs to use this technique, the protocol should also be available for MicroManager and MetaMorph softwares. This protocol is too specific to the particular microscope and software of the authors. An effort should be made to allow users with different setups to use it.

We agree with the reviewer that developing a micropatterning protocol optimized (or even compatible) with an open-source imaging software like MicroManager would be extremely useful for the cell biology community. Unfortunately, neither MicroManager nor Metamorph support any laser scanning microscopes (including multi-photon microscopes). To the best of our knowledge, every commercial laser scanning system from the Big Four microscope manufactures comes with a proprietary software and is not compatible with an open-source or competitor’s software. Because of that, it is just not feasible to develop a universal, cross platform micropatterning protocol compatible with a range of commercial multi-photon systems. However, to address the reviewer’s concern and expand an application of these protocol beyond Nikon A1R+ MP imaging system, we included a description of how the overall workflow described in the protocol can be reproduced on other imaging systems. The following text was added (page 14):

“Although the macros in our protocol enable automation of micropatterning on our system, we understand that every commercial laser scanning microscope comes with their own proprietary software that is rarely compatible with others, making it difficult to implement our exact protocol on other systems. However, the overall workflow can be well adapted to other commercial systems to facilitate automated micropatterning, namely the process of focusing on each individual FOV, loading the mask, ablating PVA, and moving the microscope stage to a new FOV.”

Temperatures must have sign (+4°C instead of 4°C)

As the reviewer suggested, we added the sign to temperatures throughout the manuscript.

Repository is missing a LICENSE file along with a copyright stated in the files.

We apologize for missing the license file for provided scripts. The license was added to the repository.

The README.md is missing installation and usage instructions.

We appreciate reviewer's suggestion to provide installation and usage instructions in the Readme.md file. The file now includes an overview of the scientific question and technique, a description of the macros and .py scripts, an explanation of the workflow, and detailed explanations of how to use the codes. Due to the syntax of the README.md file, we do not quote the updated file here but refer the reviewer to the Github repository.

No requirements.txt nor Pipfile.lock are provided, making installing the required dependencies hard. Dependencies must be listed in such file and instructions must be given on how to make the code run in a virtual environment. Along with version lock.

As the reviewer suggested, we added a requirements.txt file that includes usage instructions and the version of all packages used.

Python code MUST use the pathlib.Path python library to work well on all operating systems instead of assuming Windows path separators.

As the reviewer suggested we revised the script. The updated script uses pathlib.Path library to construct filenames.

Stage_Movement file is missing an extension and contains hardcoded paths that might not work everywhere. Paths should be configurable at the beginning of the file. Same with Pattern_Simulation: remove the hardcoded path and make it clear that this needs to be adjusted. If possible, make the application ask the user to input a file path through a GUI interface.

As the reviewer suggested, we simplified the layout of macros by defining all hardcoded variable right at the beginning of the macro. We also clearly identified hardcoded variables and changed their names to make variables self-explanatory. The section of 'Stage_Movement.mac' where the hardcoded variables are defined was revised as follows (lines 5-13):

```
“//Hardcoded Variables  
//The provided macro creates a micropatterned array of 5x5 fields of views located next to each  
//other. These values (PatternLength, PatternHeight, StepSize) are hardcoded and should be  
//adjusted if an array of different size is required. Two other input parameters required for the  
//macro are file path of a desired pattern ablation protocol and file path of a binary map of the  
//pattern. These parameters can be either hardcoded or provided through GUI (the default  
//option).  
  
int PatternLength = 5; //Length of the patterned array counted in fields of view  
int PatternHeight = 5; //Height of the patterned array counted in fields of view  
double StepSize = 532.48; //Microscope stage translocation between subsequent fields of view  
measured in micrometers”
```

We agree with the reviewer, that some users of this protocol might prefer to control the micropatterning macro through a graphical interface. Thus, we revised the macros and added two dialog windows allowing user to select the photoablation protocol and pattern map. We found this feature to be very handy! We greatly appreciate reviewer's suggestion to make the macro interactive.

In python files, use MACRO_CASE (uppercase with underscore) for constants and make it clear which ones can/should be edited. This part should be before any actual code. Also remove any hardcoded paths (like line 33 of Pattern_Averaging_3Channels.py).

As the reviewer suggested, we have changed the layout of python files with clearer instruction on how to change variables. Hardcoded paths have been replaced with a file selection dialog box.

Add a space after comment sign, conform to PEP8 (<https://www.python.org/dev/peps/pep-0008/#inline-comments>). It's also more readable. A tool like "black" (<https://github.com/psf/black>) can help formatting the code correctly.

As the reviewer suggested, we have added a space after each comment sign and slightly adjusted the format of the code to improve readability.

Example pattern image should be provided in the repository.

We appreciate reviewer's suggestion to provide pattern masks that we previously tested. Two masks of different shape and size are now available in the repository.

Reviewer 2:

Photomicro patterning using PVA-coating and multi-photon microscopy was introduced in 2009 (J. Cell Biol., <https://doi.org/10.1083/jcb.200810041>, Current Protocols in Cell Biology, <https://doi.org/10.1002/0471143030.cb1015s45>). I found it misleading that the abstract did not mention that the current protocol is an improved version of an existing method. I would also find it appropriate to not give the technique a new name (original: "microphotopatterning" here: "laser assisted micropatterning").

We apologize for downplaying the role of seminal papers published by Dr Doyle in the current protocol. In the original submission, we have cited both papers mentioned by the reviewer, and we had no intention to neglect their contribution. In the revised manuscript we cited both papers in the abstract and highlighted their critical role in the development of our protocol. The Abstract was revised as follows:

"Micropatterning is an established technique in the cell biology community used to study connections between the morphology and function of cellular compartments while circumventing complications arising from natural cell-to-cell variations. To standardize cell shape, cells are either confined in 3D molds or controlled for adhesive geometry through adhesive islands. However, traditional micropatterning techniques based on photolithography and deep UV heavily depend on clean rooms or specialized equipment. Here we present an infrared laser assisted micropatterning technique (microphotopatterning) modified from Doyle et al. that can be conveniently set up with commercially available imaging systems. In this protocol, we use a Nikon A1R MP+ imaging system to generate micropatterns with micron precision through an infrared (IR) laser that ablates preset regions on poly-vinyl alcohol coated coverslips. We employ a custom script to enable automated pattern fabrication with high efficiency and accuracy in systems not equipped with a hardware autofocus. We show that this IR laser assisted micropatterning (microphotopatterning) protocol results in clear patterns to which cells attach exclusively and take on the desired shape. Furthermore, data from a large number of cells can be averaged due to the standardization of cell shape. Patterns generated with this protocol, combined with imaging and analysis, can be used for relatively high throughput screens to understand molecular players mediating the link between form and function."

We understand the reviewer's concern with using a new name for the established technique, but we would like to keep this name as it is much more specific than "microphotopatterning" first introduced by Dr. Doyle. With the current development of new photopatterning techniques using various laser sources, we feel that microphotopatterning would not be specific enough a name for the presented technique. However, to avoid any confusion and recognize the contribution of the microphotopatterning technique to this protocol, we have used both the new and old name throughout the manuscript.

The main difficulty of this protocol is to set up the 2-photon microscope to do something 2-photon microscopes are not normally used to do. The authors provide a very detailed step-by-step protocol for their "Nikon A1R MP+" and Nikon's software package "NIS". Many of the steps describe the use of sub-menus/functions of NIS, i.e. they are very specific for this particular configuration and its version. Similarly, the necessary macros, which the authors provide, are written for NIS. Therefore, the protocol might be useful only for researchers with access to a very similar, if not identical system. Updated versions of NIS might also require changes to the protocol. In its current form, the compatibility of the protocol with 2-photon microscopes of other manufacturers is not discussed and unlikely to be easily transferable. The summary states "This user friendly technique can be set up with commercially available imaging systems". - Unless protocols for other commercial platforms are provided, it would seem suitable to me to mention in title and/or abstract that this protocol is for use with a Nikon A1R MP+ controlled NIS.

We agree with the reviewer that the provided protocol is tailored for a multiphoton microscope controlled by a proprietary Nikon software NIS Elements, but we want to draw the reviewer's attention to the fact that NIS Elements is probably the most open platform on the market. With no intention to advertise Nikon products and no financial interest in sales, we would like to highlight a wide range of third-party microscope components supported by NIS Elements (<https://www.microscope.healthcare.nikon.com/products/software/nis-elements/compatibility>). The macros we developed would run on a NIS Elements-controlled microscope equipped with a motorized stage from any major manufacture (Prior, ASI, or Ludl, etc.), a stepper-motor and/or piezo Z drive from Prior, ASI, Physik Instrumente, or Mad City Labs, an IR laser from Coherent or Spectra-Physics. These macros will literally require no modifications - the device control functions embedded in NIS Elements work with all supported hardware. Thus, we are confident that the described protocol is compatible with any multi-photon microscope controlled by NIS Elements.

While we were developing this protocol, we were also concerned with its compatibility with future versions of NIS Elements. We really like this micropatterning technique and we want to keep it in the lab toolbox and use for multiple projects. Because of that, we decided to minimize the use of device control functions in the macros and use Optical Configurations instead. If new device settings (e.g., dwell time, scan size) are available, the users will be able to implement them, if needed, through a simple and user-friendly graphical interface rather than to modify a myriad of individual functions in the macros. We also put some effort to maximize the use of relative units in the protocol (e.g., maximum zoom, fastest scan speed, smallest scan size), which we believe will make implementation of this protocol for future models of confocal scanners easier for the users. Finally, to expand an application of these protocol beyond Nikon A1R+ MP imaging system, we included a description of how the overall workflow described in the protocol can be reproduced on other imaging systems. The following text was added on page 14:

"Although the macros in our protocol enable automation of micropatterning on our system, we understand that every commercial laser scanning microscope comes with their own proprietary software that is rarely compatible with others, making it difficult to implement our exact

protocol on other systems. However, the overall workflow can be well adapted to other commercial systems to facilitate automated micropatterning, namely the process of focusing on each individual FOV, loading the mask, ablating PVA, and moving the microscope stage to a new FOV."

Another concern regarding this technique is that maintenance of multiphoton systems is costly, resulting in imaging facilities charging significant hourly fees. Since a 3.5x3.5mm area takes about 3h of patterning time, not including set-up time, this might discourage widespread use of this protocol, unless a suitable multiphoton system can be easily accessed.

We agree with the reviewer that a multi-photon microscope is not the most affordable imaging equipment and facility fees for these instruments are usually quite substantial. Nevertheless, for many labs micropatterning is the only option to manipulate cell shape. From our experience, multi-photon microscopes are much more available for a generic cell biology lab than micropatterning devices. They also require less training and easier to operate for the lab staff. In the discussion (page 14), we explain that this technique can expand the pool of multiphoton users:

"In fact, as multiphoton microscopes are becoming a more common sight in Biology departments, micropatterning expands the applications of the multiphoton microscope and adds to the potential pool of users."

Speaking from experience, our lab has access to a photolithography facility, but we rarely make PDMS stamps for microcontact printing as micropatterning is more suited for our current research needs. Therefore, we decided to provide a fair comparison of the patterning methods available for cell biologists in the introduction section of the manuscript and allow the readers to choose the most appropriate technique based on their research, equipment availability, personal preferences, etc. In addition, we suggest in the manuscript that finetuning autofocus or decreasing the number of z-plane stimulations can significantly decrease the time required. To clarify, we added the following text on page 15:

"Since IR stimulation is the most time-consuming step, the addition of each stimulation event (~30 sec) significantly lengthens the patterning process. If time is of concern, we suggest fine tuning autofocus by decreasing step size. This facilitates the identification of the best focal plane which will decrease the number of IR stimulation events required. In our experiments, decreasing the number of stimulation events from five to two reduces the time by half (1.5 h)."

The abstract mentions that "traditional micropatterning techniques based on photolithography and deep UV require clean rooms or specialized equipment", and in the introduction it is stated that "...deep UV light sources are not readily accessible in Biology departments and require special training to handle." There are in fact small deep UV light sources available for deep UV-based micropatterning that are quite affordable and do not require any specialized training (such as the ones sold by "4Dcell").

We appreciate the reviewer's insight on this matter. We have softened the statement to include such information and pointed out the advantages of our protocol with respect to this method. The following text was added on page 2-3:

"This method avoids the use of cleanrooms and photolithography equipment and requires less specialized training. However, the requirement for photomasks still poses a substantial hurdle for experiments that require readily available changes in patterns."

The current protocol uses a 25x water dipping lens. What other lenses/configurations is the protocol compatible with (immersion type, magnification, etc.)?

We appreciate reviewer's suggestion to discuss the selection criteria for the microscope objective. In fact, we believe such Note in the protocol would be extremely helpful as many imaging facilities provide multi-photon microscopes equipped with one or two objectives only. Thus, we added the following Notes on page 4-5 and 8:

"3.1. Turn on the microscope software. Ensure that the "Apo LWD 25X/1.10W DIC N2" objective is mounted on the microscope.

NOTE: *The protocol described here is optimized for a 25x/1.1 NA water immersion objective, but other objectives can also be used for patterning. Readers should be aware that patterning with a high-magnification objective (e.g., 40x and 60x) takes longer time as it significantly decreases the number of patterns ablated in each FOV. Low magnification objectives can be used for patterning as long as they provide uniform illumination across the FOV and laser power sufficient to ablate the PVA layer."*

"5.4. Lower the objective and add water onto the coverslip.

NOTE: *The protocol described here is optimized for a 25x/1.1 NA water immersion objective. If a dry or oil immersion objective is used, water should be replaced with an appropriate immersion media. When a water immersion objective is used to generate a large micropattern array, evaporation might become an issue. If this is the case, water should be replaced with GenTeal, an over-the-counter eye lubricant available from pharmacies."*

Section 1.6: The link provided for a necessary instrument, a coverslip spinner box (Section 1.6), is broken.

We apologize for the dead link for the coverslip spinner description. The link in the revised manuscript was updated as follows (page 4):

"1.6 Spin dry coverslips for 30 s using a custom-built coverslip spinner. A detailed description of the coverslip spinner has been published{Inoué.Spring.1997} and is available online (<https://mullinslab.ucsf.edu/home-built-coverslip-drierspinner/>). Activated coverslips can be stored for up to one month at +4 °C in a box with dividers so that they stand apart from each other."

Section 2 - PVA coating. Since the coverslips are immersed in solutions throughout their preparation process, are they in fact coated with PVA on both sides, but only the side facing away from the objective lens is being micropatterned? If yes, does the presence of PVA affect the optical properties of the coverslip? Can they subsequently be used on microscopes with oil-immersion lenses without damaging them?

We have never observed an ablation of the PVA layer on the surface facing the objective. We are confident that both surfaces of the coverslips are coated with PVA, but only one of them (the one we focus on) is patterned. We would expect an objective with extremely low NA to allow us patterning on both surfaces, but the output power of our laser is not sufficient to test it experimentally.

We routinely image cells attached to regular coverslips and PVA-coated patterns using dry, water- and oil-immersion objectives and we did not notice any difference in image quality that can be attributed to the PVA layer. We believe that thin layer of PVA (with a thickness of about 1/3 of the excitation wavelength for GFP) has very little impact on beam propagation through the coverslip. We also did not

notice any damage of the oil-immersion objective lenses – the chemical link between PVA and glass surface through APTMS and glutaraldehyde seems to be stable enough to sustain immersion oil. The following Note was added on the page 9 to clarify to the readers that PVA layer on the coverslips does not affect their optical properties and allows imaging with a wide range of objectives:

“Although both surfaces of the coverslip are coated with PVA, the optical properties are not significantly altered. We routinely image such coverslips with dry, water- and oil-immersion objectives and did not find the non-patterned PVA surface to interfere with imaging.”

The cover letter appears to belong to a different manuscript.

We apologize for submitting a wrong cover letter with the manuscript.





